THE UNIVERSITY of ADELAIDE

bushfire&natural HAZARDSCRC

bnhcrc.com.au

FINAL REPORT: SEISMIC RETROFIT TESTS OF URM CAVITY WALLS

Derakhshan, H., Lucas, W., Visintin, P., and Griffith, M.
School of Civil, Environmental, and Mining Engineering, University of Adelaide
Bushfire and Natural Hazards CRC

Version	Release history	Date
1.0	Initial release of document	19/7/2017

Australian Government
Department of Industry, Innovation and Science

Business Cooperative Research Centres Programme

Publisher:
Bushfire and Natural Hazards CRC

July 2017

Citation: Derakhshan, H., Lucas, W., Visintin, P., and Griffith, M. (2017) Final report: seismic retrofit tests of URM cavity walls. Bushfire and Natural Hazards CRC, Melbourne.

Cover: Building damage during the 2011 Christchurch, New Zealand earthquake. Photo: John McCombe, New Zealand Fire Service

Executive summary

University of Adelaide researchers were engaged by Bushfire and Natural Hazards CRC to undertake an experimental campaign aiming to identify and develop seismic retrofit methods for out-of-plane loaded cavity walls. The research is a part of a broader project titled "*Project A9: Cost-effective mitigation strategy development for building related earthquake risk*". This report presents the details of the tested cavity walls, trialed retrofitted schemes, obtained results, and discussion. The report concludes with recommendations on the seismic retrofit of this type of wall construction.

A review of the masonry literature suggested that retrofit methods have already been developed and widely researched for solid unreinforced masonry (URM) walls, but that the methods cannot be readily applied to cavity walls due to the cyclic nature of the seismic loads and the limited access to the cavity gap. The methods generally require access to both faces of the wall to attach fiber-reinforced-polymer (FRP) strips to masonry.

The broad retrofit concept for cavity walls was conceived to be using NSM FRP technique on the exposed surfaces of the cavity wall skins, e.g. to one face of each wall skin, but with the provision that the wall ties be verified/upgraded to maintain the cavity gap. For this purpose, 6 different alternatives of cavity structure were investigated. Two options involved the use of standard wall metal ties with different densities. Two other options included the use of proprietary helical mechanical anchors with different densities, and finally two configurations of expanding foam was used to partly or wholly fill the cavity gap. All of the FRP strips were near-surface-mounted (NSM).

It was found that with NSM FRP retrofit, the existing wall ties may be sufficient to maintain cavity gap depending on the location of the wall in Australia. For walls in regions with relatively higher seismic hazard, helical anchors can be added, and the anchor spacing can be proportional to seismic hazard but need not be less than 260 mm, i.e. every 3rd course.

Acknowledgements

The authors gratefully acknowledge the financial support of the Australian Research Council through its Cooperative Research Centre programme and specifically the Bushfire and Natural Hazards CRC.
The authors also gratefully acknowledge the technical support from the University of Adelaide Chapman Laboratory.

The views and opinions expressed in this report are those of the authors and not necessarily those of the sponsors.

Table of Contents

List of figures

List of tables

1. Introduction

The seismic vulnerability of unreinforced masonry (URM) walls to out-of-plane loading is widely acknowledged. Much research has been undertaken to develop practical techniques to provide adequate flexural strength for these URM walls which are often an integral part of the gravity load resisting structure. In solid URM walls, the surface treatments that provide tensile capacity to the wall have been shown to be very effective flexural retrofit techniques. As of late, the use of Carbon FibreReinforced Polymer (CFRP, or FRP) strips to retrofit concrete (De Lorenzis and Teng, 2006; Khalifa, 2016; Oehlers et al., 2015) and masonry (Hamed et al., 2010; Griffith et al., 2013; Kashyap et al., 2011; Kashyap et al., 2012; Ghobarah and Galal, 2004) structures have been gaining attention as a possible alternative to other existing surface treatments. In terms of application, Near Surface Mounted (NSM) and Externally Bonded (EB) FRP have gained particular interest, with both methods seeming to improve upon drawbacks associated with existing techniques such as increased mass and reduced durability, whilst having improved aesthetics and ease of installation (Korany and Drysdale, 2006).

Cavity wall construction, on the other hand, has received little attention (Walsh et al. 2015) and surface treatments are not possible to the inner faces of the two leaves of construction. Previous earthquake observations have shown that cavity masonry walls are particularly vulnerable to out-ofplane failure (Ingham and Griffith 2011) particularly is aged construction with corroded wall ties (Griffith 1991).

This report presents the results of a preliminary investigation into cavity wall connections with the aim of enabling surface treatments applied on the external faces of unreinforced clay brick cavity walls to work under full reverse cyclic loading. In these experiments NSM FRP is utilized to provide tensile strengthening of the cavity wall while, a second system is employed to maintain the cavity gap. A range of alternatives for the latter system are investigated, and the choices include expanding foam applied in the cavity with different configurations, standard cavity wall metal ties with different density, and Helifix anchors. The documented experimental observations and preliminary analysis and implications of the data are reported herein, with a more in-depth analysis and interpretation of the data being published at a later time.

2. Experimental Plan

4.1. Test Plan

Nine masonry wall were tested as part of this study to investigate the effect of cavity wall connection details and the potential performance increase that could be obtained via strengthening of the cavity connection for FRP-reinforced masonry wall. The walls were 110 mm thick, 470 mm wide, and 2310 mm high. The test variables included the connection type and spacing. Table 1 shows the details and results of the walls tested as part of this research.

Table 1: Test walls*

Wall ID	Connection Details	Remarks
W1	-	Single-leaf
W2	Standard ties @ 520 mm	No FRP
W3	Standard ties @ 520 mm	
W4	Standard ties @ 260 mm	
W5	5 helical anchors** @ 430 mm	
W6	10 helical anchors** @ 430 mm	
W7	Foam infill	
W8	50 x 75 mm foam strip	
W9	50 x 75 mm foam strip	No FRP

* Unless otherwise noted under “Remarks” column, the walls were of cavity construction (with 75 mm gap), with one leaf being retrofitted using NSM FRP technique

** The anchors were proprietary Helifix anchors with inner and outer diameter of, respectively, 3 and 8 mm.

Wall 1 was a single-leaf wall that was used as a control measure to establish the strength of a single masonry leaf and hence to aid in determining the effectiveness of each connection type that was subsequently investigated. Additionally, with the exception of Walls 2 and 9, all of the walls were reinforced with a single 3 x 8 mm NSM CFRP strip (Figure 1) applied to the tensile face of one of the wall leaves. As previously mentioned the aim of this study was to investigate the influence of connections between cavity walls and any connection strengthening required in order to fully utilize the previously investigated solid wall retrofitting techniques. As such the tensile strengthening was held constant between the tests. Wall 2 was used to demonstrate the capacity of an unstrengthened cavity wall and provided a baseline for comparison with the remaining wall tests. Walls 3 and 4 were tested to investigate the effect of wall tie spacing, walls 5 and 6 to investigate the use of mechanical helical anchors, and walls 7, 8 and 9 to investigate the use of expanding foam.

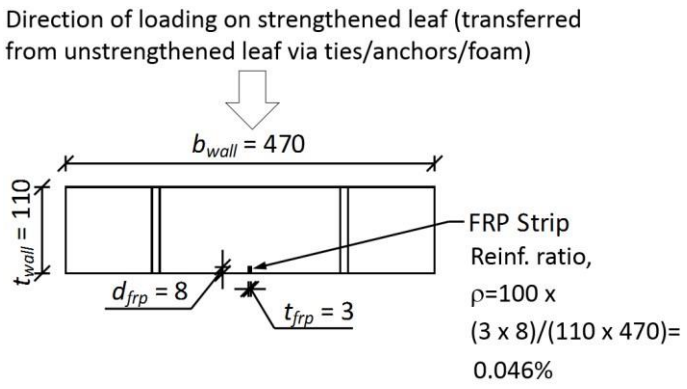

Figure 1: Typical reinforced leaf cross-section

4.2. Material Properties

The average material properties for the masonry walls and CFRP strips are listed in Table 2. The material properties in Table 2 were tested in accordance with AS3700 and AS/NZS 4456. The walls and associated material tests were constructed over a single day by 3 qualified bricklayers operating under laboratory controlled conditions to minimize any variations in material components. The masonry units comprised of standard Australian clay bricks with nominal dimensions of 230 x 110 x 76mm and 2 rows of 5 perforations (Figure 2(a)). All masonry was constructed using brick units from the same manufacture batch. Mortar joints were nominally 10mm thick and mixed using Portland cement, hydrated lime and sand in a 1:1:6 ratio by volume. For all cavity walls red galvanized double legged wall ties 230 x 3mm in size (Figure 2(b)) were utilized.

Table 2: Material Properties

Material Property	Mean (MPa)	Standard Deviation (MPa)	Coefficient of Variance (%)
(Masonry)			
Flexural tensile bond strength, f_{mt}	0.45	0.12	27
Modulus of rupture of brick units, f_{ut}	2.61	0.20	8
Masonry compressive strength, f_{mc}	13	1.58	12
Compressive strength of mortar joints	8	0.5	7
Masonry strain at f_{mc}, ε_{mc}	0.0024	0.0007	18
Elastic modulus of Masonry, E_m	10,000	1,500	15
Elastic modulus of masonry units, E_u	22,555	2,350	10
Elastic modulus of mortar, E_j	6,100	2,400	39
(CFRP)			
Ultimate tensile strength, f_{rupt}	1,800	32	2
Elastic modulus, E_{frp}	158,000	1,300	1

4.3. Specimen Design

Each wall specimen was constructed with nominal dimensions as shown in Table 1 and Figure 3 to Figure 5. The NSM FRP strips were aligned vertically along the central line of the wall such that the FRP strip ran through the perpend joints at alternate brick courses. This method minimizes the visual impact of the FRP strengthening technique and hence is a likely method for use in practical application. Running the strip through the perpend joints has previously been shown to have minimal impact on the IC debonding load (Willis et al., 2009). The FRP retrofitting scheme was designed using partialinteraction theory (Kashyap et al., 2012) such that IC debonding was the tensile failure mode rather than rupture of the FRP strips. It should also be noted that the tested specimens, with the exception of Walls 1 and 7, were expected to experience failure of the cavity connection, either in the form of foam compression or tie/anchor buckling/punching failure, prior to complete IC debonding. The FRP strips were manufactured in a single batch to the 3 x 8 mm dimensions via the method of pultrusion. Following delivery the strips were lightly sanded and cleaned with acetone prior to installation to remove any foreign substances that may be present in the surface layer of the FRP strip. The groove for the FRP strip was cut using a diamond blade circular saw and cleaned with a high-

pressure air jet. The groove was subsequently filled with the epoxy adhesive into which the FRP strip was inserted such that it was flush with the masonry surface.

(a) Perforated clay brick (b) 3 mm thick wall ties; inset shows the bent shape as used in walls Figure 2: Standard masonry units and wall ties

The walls comprised of three difference cavity connection types as follows:

Standard wall ties (W2, W3, W4) Figure 3: These connections were installed during construction of the masonry cavity walls by placing into the mortar joints between the brick courses at regular intervals. For walls W2 and W3 the vertical tie spacing was 520mm while for wall W4 this spacing was reduced to 260mm.

Helical anchors (W5, W6) Figure 4: The helical anchors were retrofitted to the wall prior to testing. In all cases existing wall ties were cut such that the helical anchors provided the sole connection across the cavity. Installation involved drilling a pilot hole through the reinforced wall leaf, through the center of a brick unit, and 75mm into the loaded leaf. The helical wall anchors were then pushed into the wall using an SDS type hammer drill. For wall W5 one anchor per level was installed at 430mm vertical spacing, 40mm offset from the NSM FRP strip on alternating sides per level. For wall W6 the vertical spacing remained constant at 430mm, however, each layer involved the installation of 2 anchors. Each anchor was installed 80mm from each side of the masonry wall.

Expanding Foam (W7, W8, W9) Figure 5: Expanding foam was inserted into the cavity prior to testing. In all cases existing wall ties were cut such that the foam provided the sole connection across the cavity. For wall W7 installation involved mixing the 2 part liquid components and pouring into the wall cavity. In the case of W7 the entire cavity was filled (Figure 5(c)) with foam over 3 pours of approximately 1/3rd of the wall height. In the case of W8 and W9 50mm vertical strips of foam were installed at each side of the wall using canned foam. Installation involved installing piece of thin cardboard the full height of the wall inset a nominal 50mm from the wall edge (Figure 5(d)). Foam was then sprayed into the channel and left to expand. Once the foam had fully expanded any excess foam was cut from the wall using a hand saw.

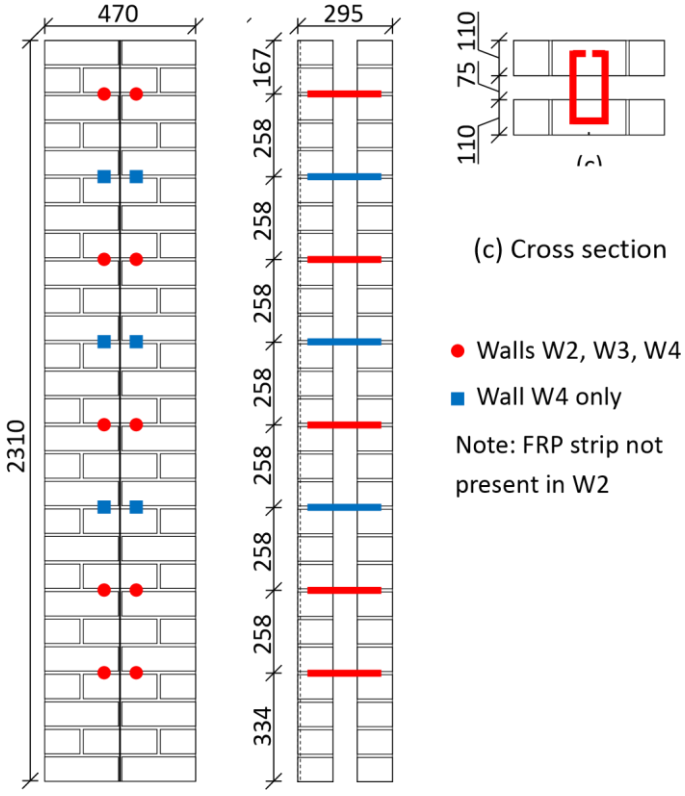

(a) Front view (b) Side view

Figure 3: Wall tie configuration

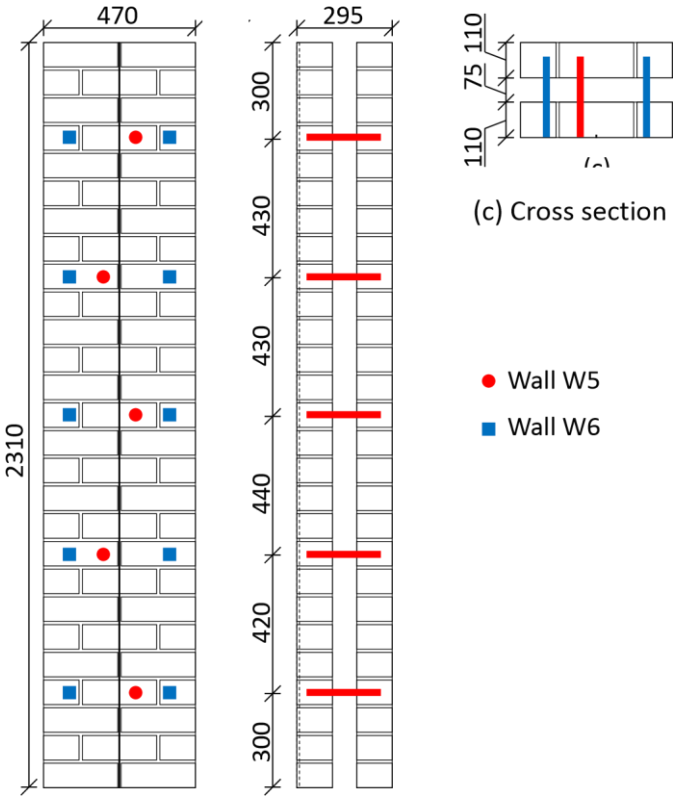

(a) Front view (b) Side view

Figure 4: Helical anchor configuration

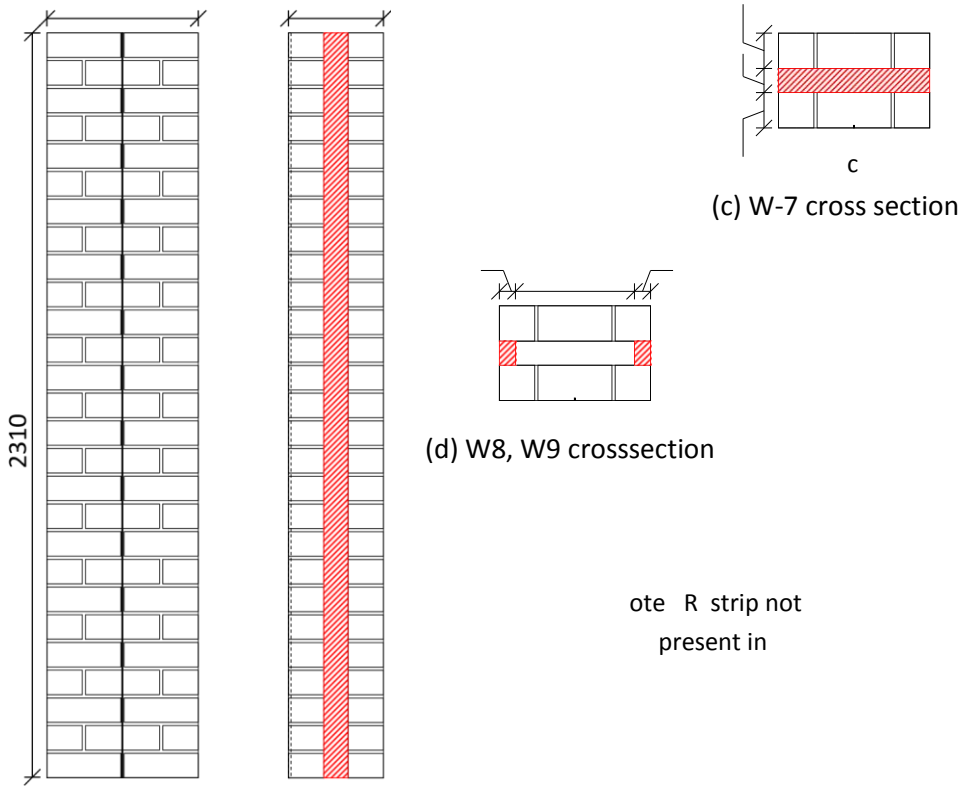

(c) W-7 cross section

(d) W8, W9 crosssection

ote R strip not present in

(a) Front view (b) Side view

Figure 5: Foam infill configuration

4.4. Test Setup and Instrumentation

The test walls were constructed on smooth timber supports to minimize base friction while maintaining a stable construction surface. The walls were restrained from lateral movement via roller supports located at the second courses from the top and bottom of the FRP reinforced wall leaf (Figure 6(d)). All test walls were subjected to a uniformly distributed applied load via an airbag placed between the test wall and the adjacent reaction frame such that the FRP strip was placed into tension. The pressure in the airbag was slowly increased via a manually controlled air valve. The typical test wall setup and reaction frame is shown in Figure 6(a).

To document the wall response a combination of 26 Linear Variable Displacement Transducers (LVDTs), 2 strain gauges and 1 pressure transducer were utilized. The instrumentation locations were kept constant for all experimental testing.

Two 10mm strain gauges were glued directly onto each FRP strip at the mortar joint closest to the mid-height of the masonry wall (Figure 7) and a clear plastic film used to prevent the strain gauge from bonding to the adjacent masonry. The strain gauges were installed at a mortar joint, to minimize any loss in bond strength between the FRP and masonry.

The 26 LVDTs were installed at various wall heights to capture the deflected shape profile of the reinforced leaf, the change in the cavity dimension (subsequently providing the deflected shape profile of the loaded leaf) and the flexural crack widths near the mid-height of the masonry wall (Figure 6(b) and (c)). Table 3 below documents the height of the installed face and side LVDTs. The 6 LVDTs configured to record the crack width opening were positioned at mid-height covering the 11^{th} to 17^{th} brick courses.

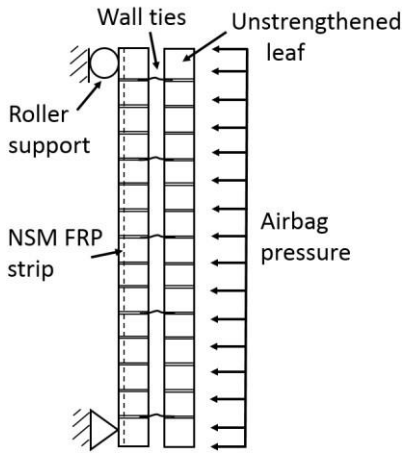

(a) Schematic of the setup

(b) Typical test setup

(c) Front LVDT and crack width LVDTs

(d) LVDT to monitor changes in the gap

(e) Bottom view of the top roller support Figure 6: Test setup

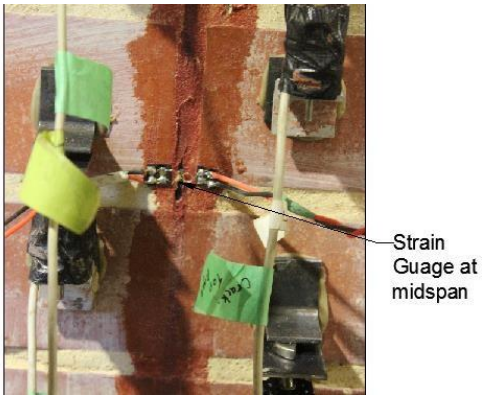

Figure 7: Instrumentation to the strain gauge mounted on FRP strip at mid height Table 3: Face and side installed LVDT heights

LVDT Location	Brick Course	Nominal height relative to base of wall (mm)
Above lower roller support	3	205
1 quarter height	8	665
Mid-height	14	1180
3 quarter height	20	1670
Below top roller support	25	2070

3. Results

The wall test results are summarized in Table 1, where σ_{max} refers to the maximum distributed load applied to the wall and Δ is the mid-height displacement of the reinforced leaf when σ_{max} was achieved. The following sections provide detailed discussion on each of the wall tests undertaken.

Table 4: Summary of the measured peak wall strength and the associated maximum displacement

Peak strength, σ_{max}	Mid-height (maximum) displacement at peak strength Δ at σ_{max}
kPa	mm
17.2	61.4
2.0	2.2
8.7	26.3
12.1	44.0
7.7	25.4
14.4	60.7
24.9	16.8
18.9	40.1
4.1	9.1

5.1. W1 - Single Leaf

Testing of the single leaf wall was undertaken on the 26th of February 2016 in the Chapman Laboratory at The University of Adelaide. The general test setup for the single leaf wall was similar to that shown in Figure 6 except that the wall was single-leaf and the airbag loading was applied directly to the unstrengthened face of the wall. The instrumentation was placed as per Table 3 with the exception that the side LVDTs were not required due to the lack of a second leaf. The single leaf test utilized the same reaction frame as the cavity wall tests and hence an additional timber packing frame was installed between the airbag and the reaction frame.

The purpose of the single leaf test was to provide a baseline strength for the reinforced wall leaf. By comparing the cavity wall specimens strength with the single leaf scenario it was possible to determine how well the retrofitted surface treatment technique was activated by the various cavity connections and hence it was possible to compare the effectiveness of the investigated connection types.

Figure 8(a) shows the load to mid-height deflection profile for the single leaf wall. At an applied pressure of 1.7 kPa a horizontal crack formed along the brick unit to mortar interface between the 14th and 15th courses. Figure 8(a) shows that the formation of this first crack coincides with a significant change in the load-deflection behavior which is caused by the reduction in sectional stiffness.

If the wall had not been reinforced with the NSM CFRP strip ultimate failure of the wall would have occurred shortly after the formation of the first horizontal crack as the wall rotates about this crack location under increasing displacements. Instead, as shown in Figure 8(d), as the flexural tensile strength of the masonry is exceeded the tensile forces within the member are resisted by the FRP strip allowing for further increased loading and further crack development.

Closer inspection of the mortar joints near the center height of the wall (shown in Figure 8(b)) shows that after the formation of the first horizontal crack between the 14th and 15th courses additional horizontal cracks form along the 16th to 17th, 11th to 12th, and 13th to 14th courses almost immediately.

Following this initial set of cracking small horizontal cracks were visible on the wall at approximately every second mortar joint near the wall mid-height. At an approximate pressure of 3.8 kPa additional horizontal cracks formed along the 12th to 13th, and 15th-16th courses such that small horizontal cracks were present at each mortar joint near the mid-height of the wall. This behavior is consistent with the formation of primary and secondary cracks as described within partial-interaction theory (Visintin et al., 2013).

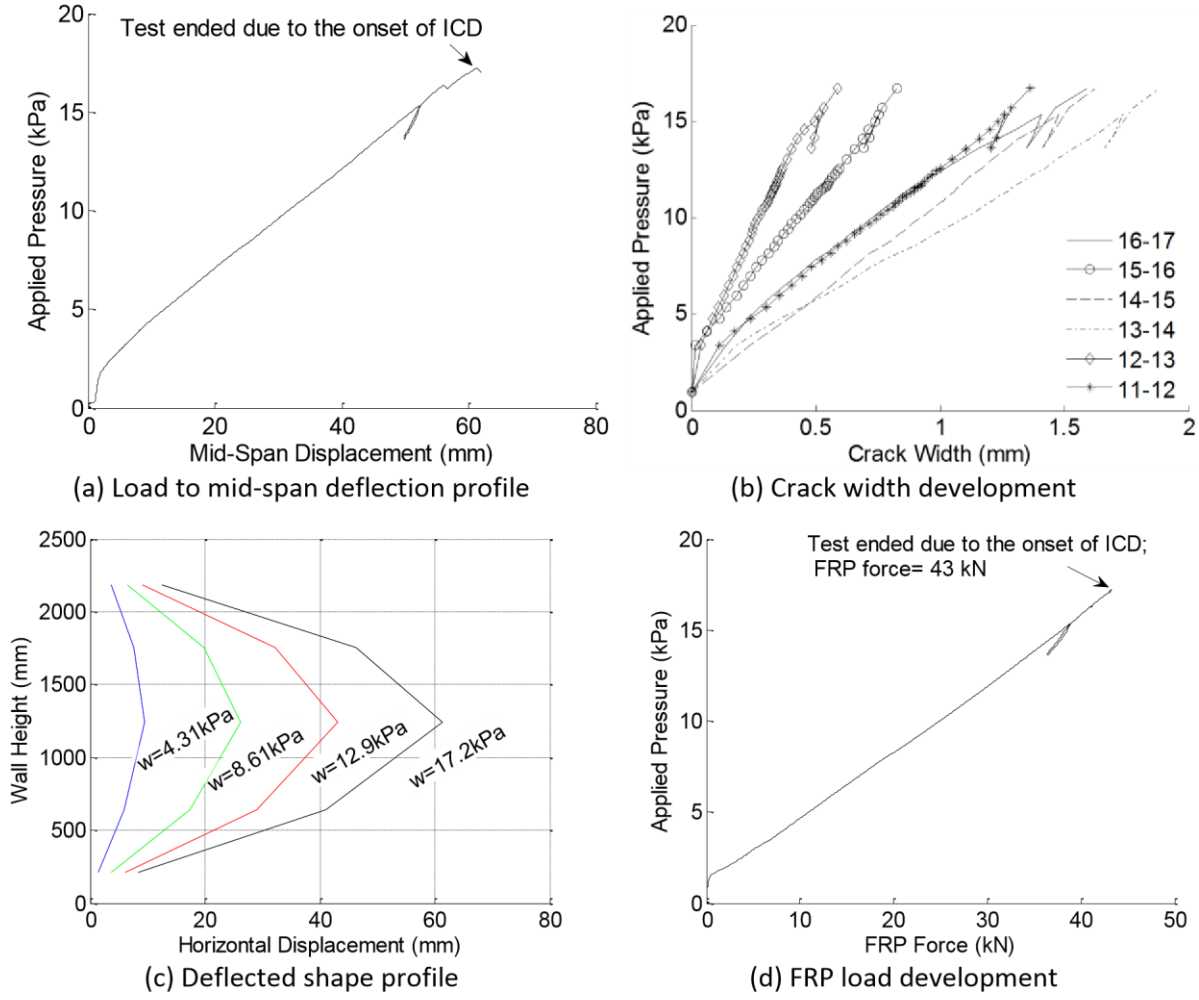

Figure 8: Wall 1 test results

Continued loading of the single leaf wall resulted in the formation of herringbone cracking (Figure 9(c)) associated with partial interaction debonding of the FRP strip. Interestingly the single leaf scenario demonstrated clear herringbone cracking on both sides of the brick unit indicating that debonding is occurring in both directions over the height of a single brick unit. This behavior is consistent with the multiple cracking scenario described in recent partial interaction studies (Oehlers et al., 2015) and the visible confirmation of this behavior is something that has not been documented elsewhere. In the case of this single leaf test, global IC debonding ultimately resulted in failure of the wall at an applied pressure of 17.2 kPa, at a pressure that was 10 times the initial cracking pressure of 1.7kPa. The global IC debonding resulted in a sudden increase in the width of the crack at the interface between the 17th and 18th brick courses as the entire FRP strip above the crack slipped approximately 30mm as shown in Figure 9(a) and (b). Interestingly the recorded crack width behavior in Figure 8(b) did not

demonstrate any evidence of the crack closure theorized (Oehlers et al., 2015) to be associated with the shift from the observed multiple crack debonding to the single crack debonding associated with the global IC debonding behavior. It is also interesting to note that in this case failure of the bond between the FRP and the brick unit did not occur within the brick unit itself which has previously been documented (Kashyap et al., 2011) but rather failure occurred within the surface layers of the FRP. This behavior was also observed in the material tests undertaken in conjunction with the wall tests. It is theorized that this failure mechanism is directly related to the fact that the FRP strips were manufactured using the pultrustion method and that it is possible that the release agent used during manufacture became mixed with the binding agent in the outer layers of the FRP strip resulting in a weak surface layer within the material itself.

Interestingly the IC debonding pressure for this NSM FRP strip was estimated from pull test to be approximately 17.5kPa. This combined with Figure 8(d) indicates that following the onset of IC debonding there was a significant increase in force within the FRP stip. This is likely caused by a combination of friction and tension stiffening behavior. The deflected shape profile shown in Figure 8(c) was consistent with the desired simply supported test configuration.

(a) Deflection profile at failure

(b) Slip of the FRP reinforcement associated with IC debonding

(c) Dual direction herringbone crack formation

Figure 9: Wall 1 final cracking pattern

5.2. W2 - Cavity Wall, Standard Wall Tie Spacing, No FRP

The 2nd wall test consisted of an unreinforced cavity wall where the connection between the masonry leaves consisted of standard wall ties spaced at every 6th bedjoint (~=520mm centers). Testing was

undertaken on the 19th of April 2016 in the Chapman Laboratory at The University of Adelaide. The general test setup for the test wall is shown in Figure 10(a).

The purpose of this test configuration was to provide a baseline strength for the unreinforced masonry cavity wall and hence determine the increase in the load and deflection carrying capabilities of the subsequent cavity tie and reinforcement configurations.

The response of the unreinforced cavity wall was dominated by the formation of 3 horizontal cracks which all occurred around an applied load of 2.0 kPa. A single crack formed in the front, unloaded leaf between the 15th-16th courses near the mid-height of the wall and the remaining 2 cracks formed in the loaded leaf between the 13th-14th and 17th-18th courses as shown in Figure 10(b). Subsequent loading resulted in increased deflections, accommodated by the growth of these 3 cracks (Figure 10(c)), with no increase in the resisted pressure.

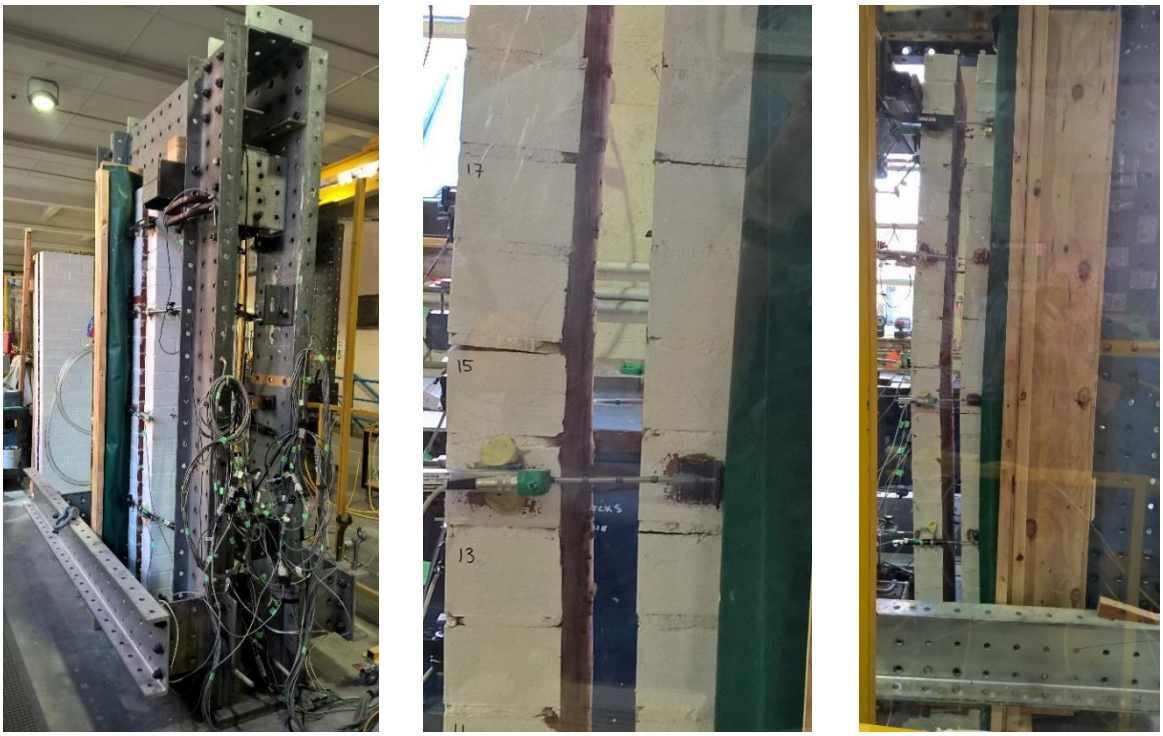

(a) General test configuration (b) Flexural crack development (c) deflected profile post maximum load

Figure 10: Wall 2 final cracking pattern

Figure 11(a) shows the load to mid-height deflection profile for the second wall test where the 'blue' line shows the mid-height deflection of the front, unreinforced leaf and the 'green' line shows the mid-height deflection of the airbag loaded leaf. It should be noted that the initial deflection prior to 2 mm was caused by a rotation of both wall leaves such that good contact was made with the top roller support at the 26th course. This initial rotation displacement was exaggerated with wall height. The initial rotational displacement has been removed from the subsequent figures. Figure 11(a) shows that the loaded leaf follows closely the path of the front, unloaded leaf and demonstrates that the wall ties were capable of maintaining the cavity width at mid-height. This observation is further highlighted in Figure 11(b) which shows that the maximum reduction in the cavity width prior to achieving the

maximum applied load was 0.2 mm at the top of the wall. Figure 11(c) demonstrates the horizontal deflection profile of the wall at various applied loads.

In Figure 11(c) the solid line corresponds to the deflection of the reinforced leaf and the dashed line shows the deflection of the loaded leaf. Once again this clearly shows that the wall ties were able to maintain the cavity dimensions up to the maximum applied load and further that the cavity width was maintained during the subsequent period of increasing deflection with reducing load. Finally Figure 11(d) shows the crack width development near mid height of the front leaf. Figure 11(d) clearly shows that the deformation of the front leaf was dominated by the growth of a single crack. This demonstrates a significant change in the behavior from the reinforce leaf in the first wall test where small cracks formed along each mortar joint.

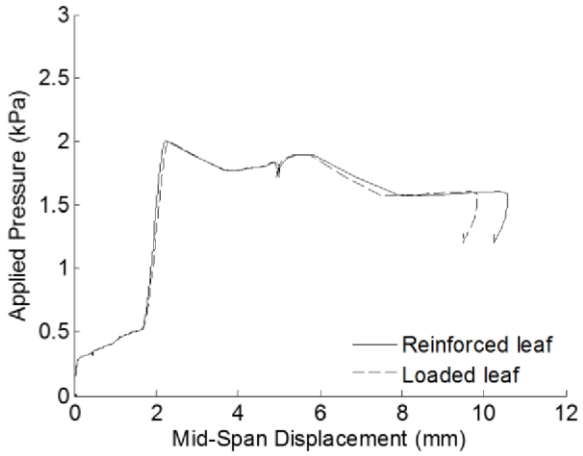

(a) Applied pressure vs mid-span displacement

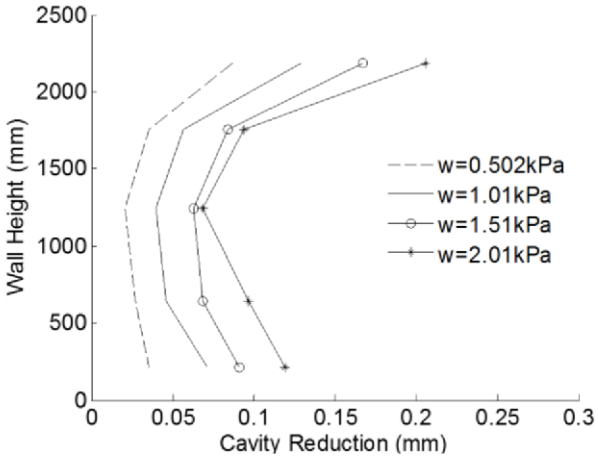

(b) Reduction in cavity width

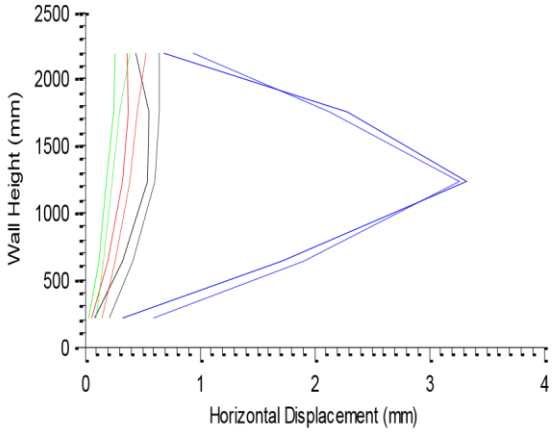

(c) Deflected shape

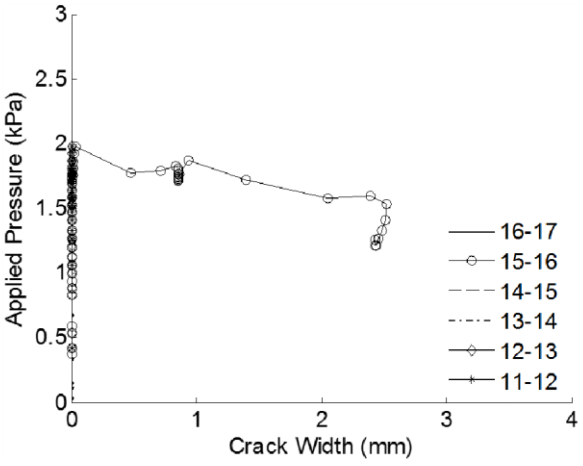

(d) Crack width development (single crack)

Figure 11: Wall 2 test results

5.3. W3 - Cavity Wall, Standard Wall Tie Spacing

In Wall 3, the connection between the masonry leaves was consisted of standard wall ties at every 6th mortar bedjoint (~= 520mm centers). Testing was undertaken on the 22th of September 2015 in the Chapman Laboratory at The University of Adelaide. The general test setup for the test wall is shown in Figure 12(a).

The purpose of this test configuration was to investigate the ability of wall ties installed in a standard configuration to transfer flexural load between masonry leaves and hence determine what utilization of any tensile R strengthening could be achieved in an existing wall with "good" wall ties.

Figure 13(a) shows the load vs mid-height deflection response for wall test where the 'blue' line shows the mid-height deflection of the R reinforced leaf and the 'green' line shows the mid-height deflection of the airbag loaded leaf. Figure 13(a) shows that the loaded leaf follows closely the path of the reinforced leaf and demonstrates that the wall ties were capable of maintaining the cavity width at mid-height. This observation is further highlighted in Figure 13(b) which shows that the maximum reduction in the cavity width prior to achieving the maximum applied pressure of 8.7 kPa was 2.3mm at three quarters of the wall height. Similarly Figure 13(c) demonstrates the horizontal deflection profile of the wall at various applied loads. In Figure 13(c) the solid line corresponds to the deflection of the reinforced leaf and the dashed line shows the deflection of the loaded leaf. Once again this clearly shows that the wall ties were able to maintain the cavity dimensions right up to the point at which buckling of the wall ties occurred. Importantly the wall ties were able to maintain a simply supported deflected shape in the loaded leaf.

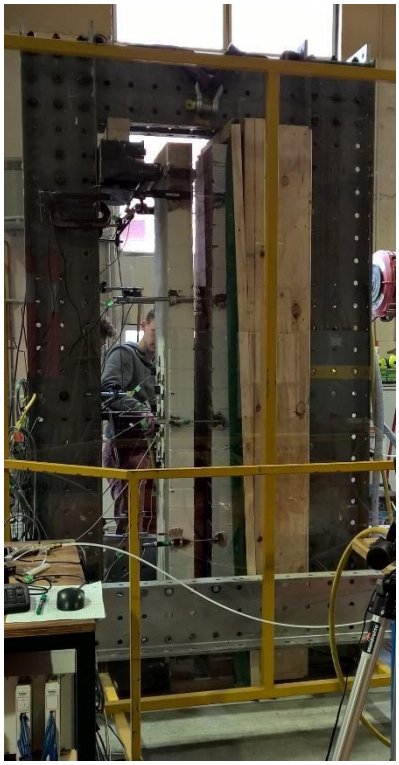

(a) General test configuration

(b) Cracking of the loaded (indicated by arrows)

(c) Buckling of the top-most wall leaf tie (pictured)

Figure 12: Wall 3 final cracking pattern

As previously observed there is a significant change in behavior of the wall around an applied load of 0.8 kN/m corresponding to initial tensile cracking of the masonry. In the case of the loaded leaf a horizontal crack first occurred in the 18th to 19th mortar joint and was followed shortly by the formation of a second crack at the 11th to 12th mortar joint (Figure 12(b)) such that the loaded leaf now behaved as 3 rigid bodies. Cracking in the reinforced leaf followed a similar pattern to that of the single leaf wall test with the formation of primary and secondary cracking such that small horizontal cracks formed at most mortar joints. As demonstrated by the recorded crack widths in Figure 13(d) horizontal

cracks formed at each of the 6 central mortar joints prior to a pressure of 4.3 kPa being applied to the wall.

Post cracking of the masonry, increased loading resulted in roughly linear deflected behavior right up to the ultimate pressure of 8.7 kPa being achieved at which point the wall ties at the 19th to 20th and 25th to 26th mortar joints buckled resulting in a sudden reduction of the cavity width (Figure 12(c)). Unfortunately failure of the strain gauges attached to the FRP strip meant that no data could be collected on the force in the FRP strip. It can be stated that at failure of the cavity connections there was no visible herringbone crack formations around the FRP strip potentially indicating that no significant debonding had been achieved.

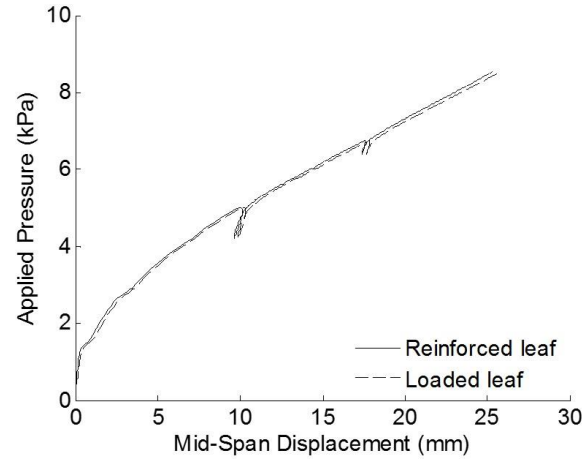

(a) Load vs mid-span displacement

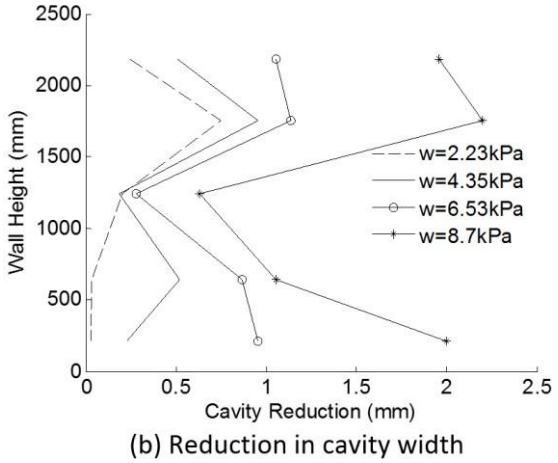

(b) Reduction in cavity width

(b) Reduction in cavity width

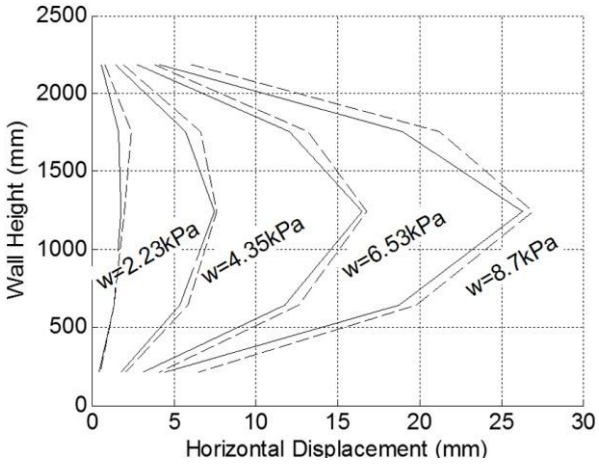

(c) Deflected shape profile

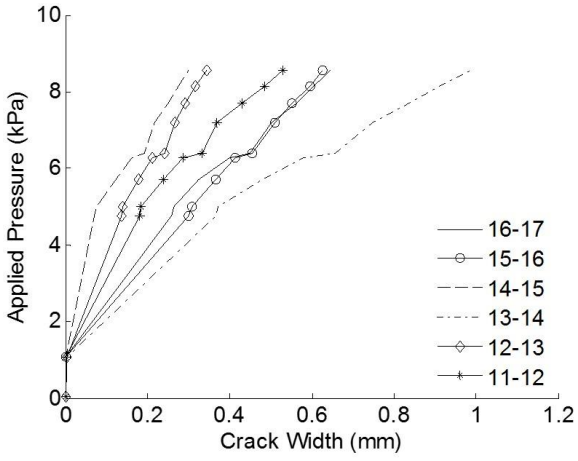

(d) Crack width development

Figure 13: Wall 3 test results

5.4. W4 - Cavity Wall, Improved Wall Tie Spacing

The 4th wall test consisted of an FRP reinforced cavity wall where the connection between the masonry leaves consisted of standard wall ties spaced at every 3rd bedjoint (~= 260mm centers). Testing was undertaken on the 11th of September 2015 in the Chapman Laboratory at The University of Adelaide. The general test setup for the test wall is shown in Figure 14(a).

The purpose of this test configuration was to investigate the increase in connection performance that could be achieved by wall ties installed in excess of the 600mm typically installed in aged buildings. It is noteworthy that the Australian Masonry Standards, AS 3700, stipulates wall tie spacing depending on the performance class of the wall tie, which includes “light duty”, “medium duty”, and “heavy duty” categories. It is generally considered that the aged buildings that are the most vulnerable to seismic forces have not been designed according to this standard.

Figure 15(a) shows the load to mid-height deflection profile for wall test 4 where the ‘blue’ line shows the mid-height deflection of the R reinforced leaf and the ‘green’ line shows the mid-height deflection of the airbag loaded leaf.

From Figure 15(a),(b) and (c) it can be seen that the decreased wall tie spacing does not appear to significantly improve the reduction in crack width with both Walls 3 and 4 demonstrating a similar 2 mm reduction at an applied pressure of 8.7 kPa. Notwithstanding, the reduced wall tie spacing does appear to improve the deflected shape profile of the loaded leaf which more closely mimics that of the reinforced leaf and resembles that of a simply supported beam (Figure 14(b)) rather than the distinct rigid bodies that formed between limited number of cracks in wall test 3 (Figure 12b). more importantly, the closely spaced wall ties resulted in improved load sharing and hence delayed the onset of buckling of the wall tie connections.

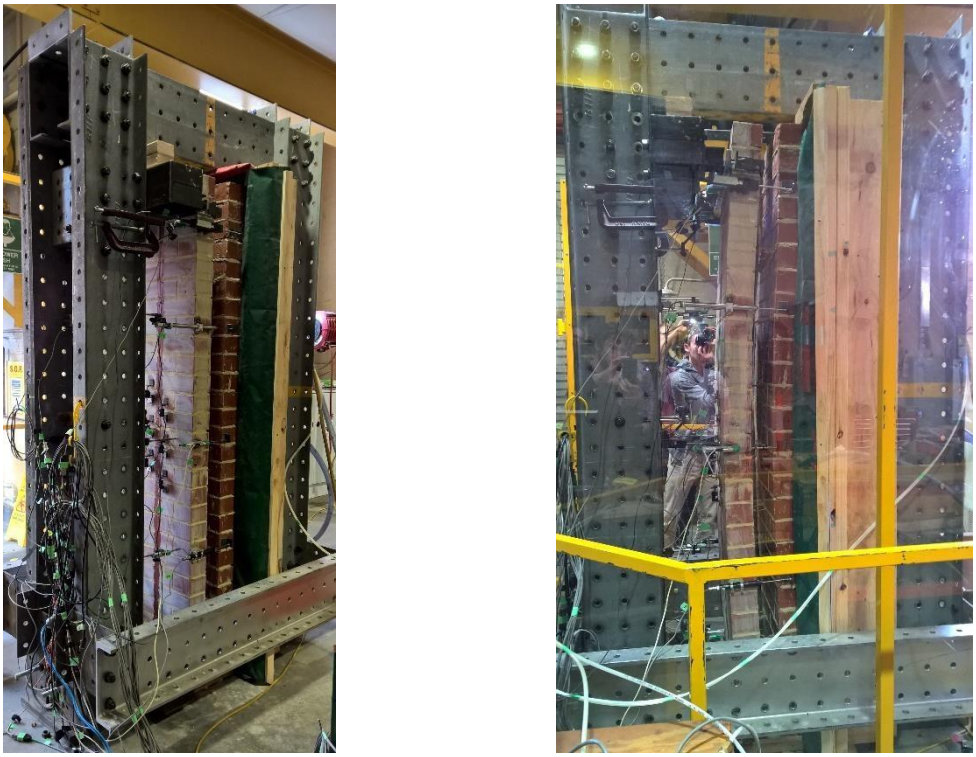

(a) Overall test configuration (b) Deflected shape profile

Figure 14: Wall 4 final cracking pattern

A significant change in behavior occurred in the wall at an applied pressure of 2.1 kPa (see Figure 15a) corresponding to initial tensile cracking of the masonry. The reduced wall tie spacing resulted in additional flexural cracks forming in the loaded leaf such that a horizontal crack formed at approximately every 4th mortar joint.

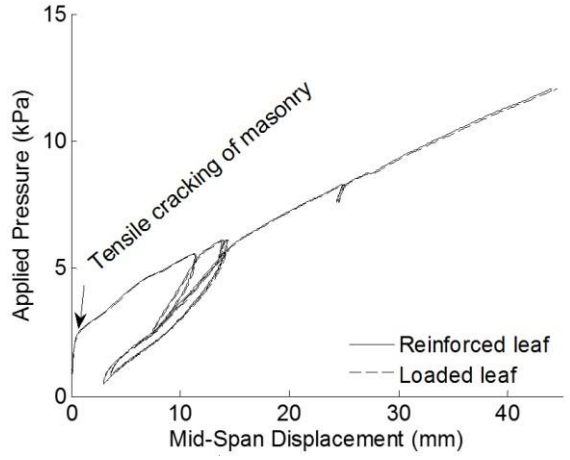

(a) Load vs mid-span deflection profile

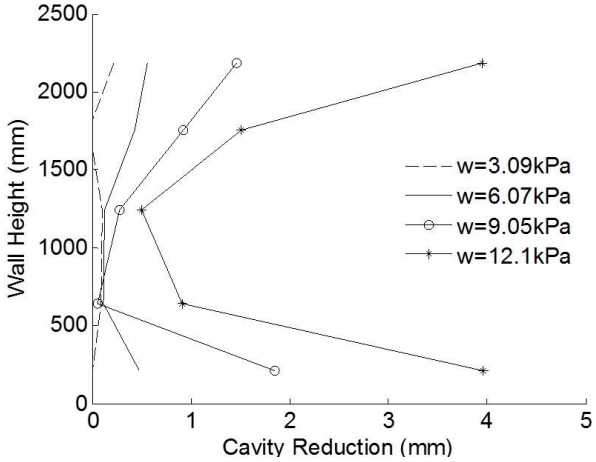

(b) Reduction in cavity width

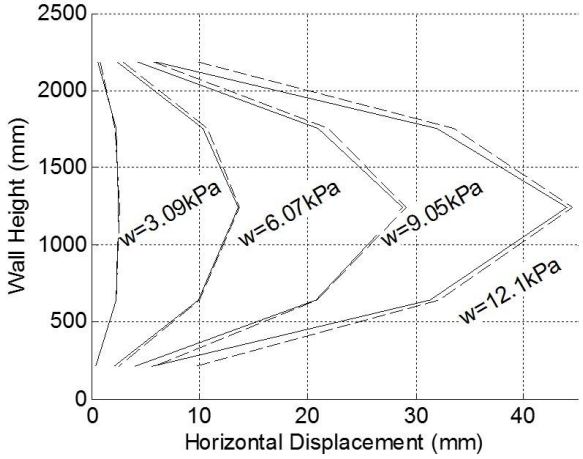

(c) Deflected shape profile

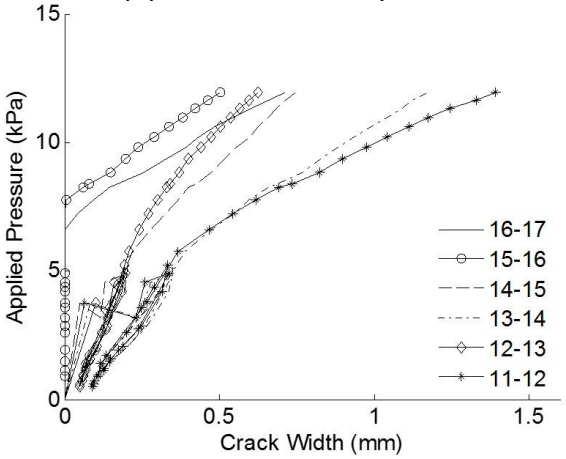

(d) Crack width development

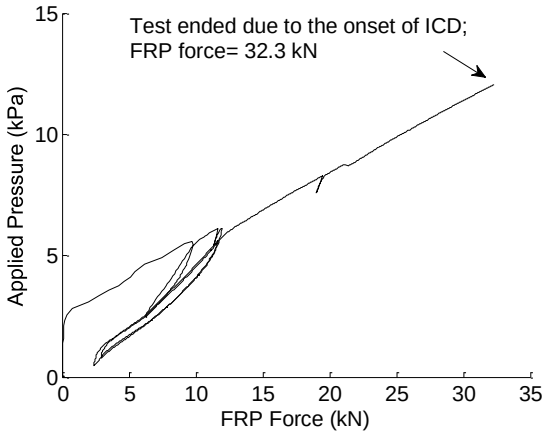

(e) FRP force development

Figure 15: Wall 4 test results

Ultimately the wall failed as a result of buckling of the wall tie at the 25th to 26th mortar joint and the formation of a complete horizontal crack through the 19th to 20th mortar joint. The failure pressure of 12.1 kPa corresponded to a 40% increase in failure load over that of Wall 3 with ties at double the spacing.

The FRP force development in Figure 15(e) would indicate that IC debonding of the reinforcement had commenced however compared with the single leaf case from Wall 1 the FRP strip had only developed

32.3 kN, which is approximately 75% of the force (43 kN from Figure 8d) required to induce IC debonding in the single-leaf Wall 1.

5.5. W5 - Cavity Wall, Mechanical Anchorage 1

Testing of the 5th Wall was undertaken on the 30th of September 2015 in the Chapman Laboratory at The University of Adelaide. The 5th wall test involved the retrofit and retesting of the wall utilized in wall test 3. Following buckling failure of the wall ties the connections were cut and both leaves returned to vertical. At this point helical wall anchors (Figure 16(a)) were driven into predrilled holes near the center line of the wall on alternating sides of the FRP strip as indicated in Figure 4(a). It is worth noting that pre-drilling the holes through the reinforced face resulted in significant conical blowout of the back face of the brick units (Figure 16(b)).

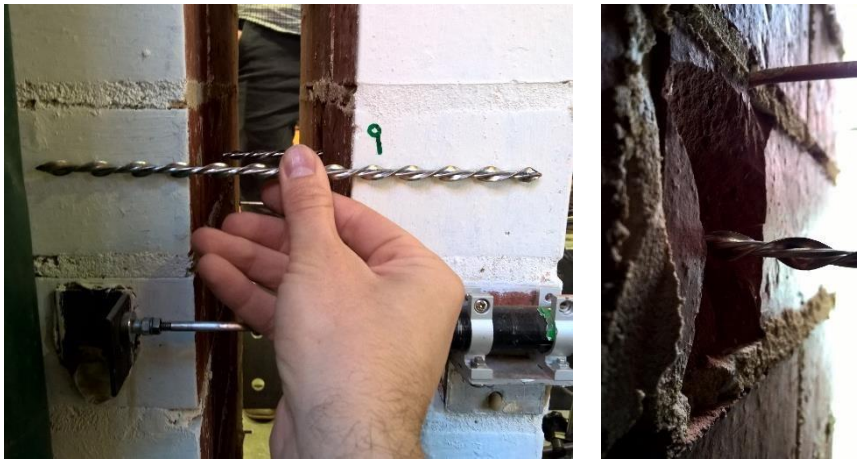

(a) Helical wall anchor (b) Blowout failure of the brick

Figure 16: Wall 5 retrofit details

The purpose of the mechanical anchorage test was to determine if, in situations where the existing cavity walls and wall ties were understrength or of unknown condition, mechanical anchorage could be added to improve the wall connection such that the benefit of tensile strengthening of the cavity walls could be utilized.

Figure 17(a) shows the load to mid-height deflection profile for wall test 5 where the 'blue' line shows the mid-height deflection of the R reinforced leaf and the 'green' line shows the mid-height deflection of the airbag loaded leaf.

It is immediately clear that significantly larger differential wall deformation was associated with the mechanical anchors, with reduction in the cavity width being greater than that in Wall 3 that had standard wall ties. Figure 17(b) and (c) show that the cavity reduced by a maximum of 16mm corresponding to a 20% reduction in overall cavity width. This was likely caused by the anchors failing to achieve a good bond with the reinforced leaf, possibly affected by the conical brick failure during predrilling or potentially the 10 perforations present in the brick units. It was observed that at completion of the test the wall anchors had been pushed 15mm out of the reinforced wall leaf such that they pultruded 10mm out of the face of the wall leaf.

Unlike the previous wall tests Wall 5 did not display the initial stiff load deflection behavior due to the pre-existing cracks existing in both wall leaves. Figure 17(d) shows that the flexural cracks near the

center of the reinforced leaf began to reopen immediately and a constant linear load-deflection behavior was observed throughout the test.

Unfortunately wall test 5 failed prematurely due to the lateral buckling of the top most wall anchor at a pressure of 7.7 kPa. The green canvas containing the air bag detached from the timber framework on the right hand side of the test wall. This resulted in the airbag wrapping around the edge of the test wall and applying an additional lateral load leading to premature buckling of the anchors.

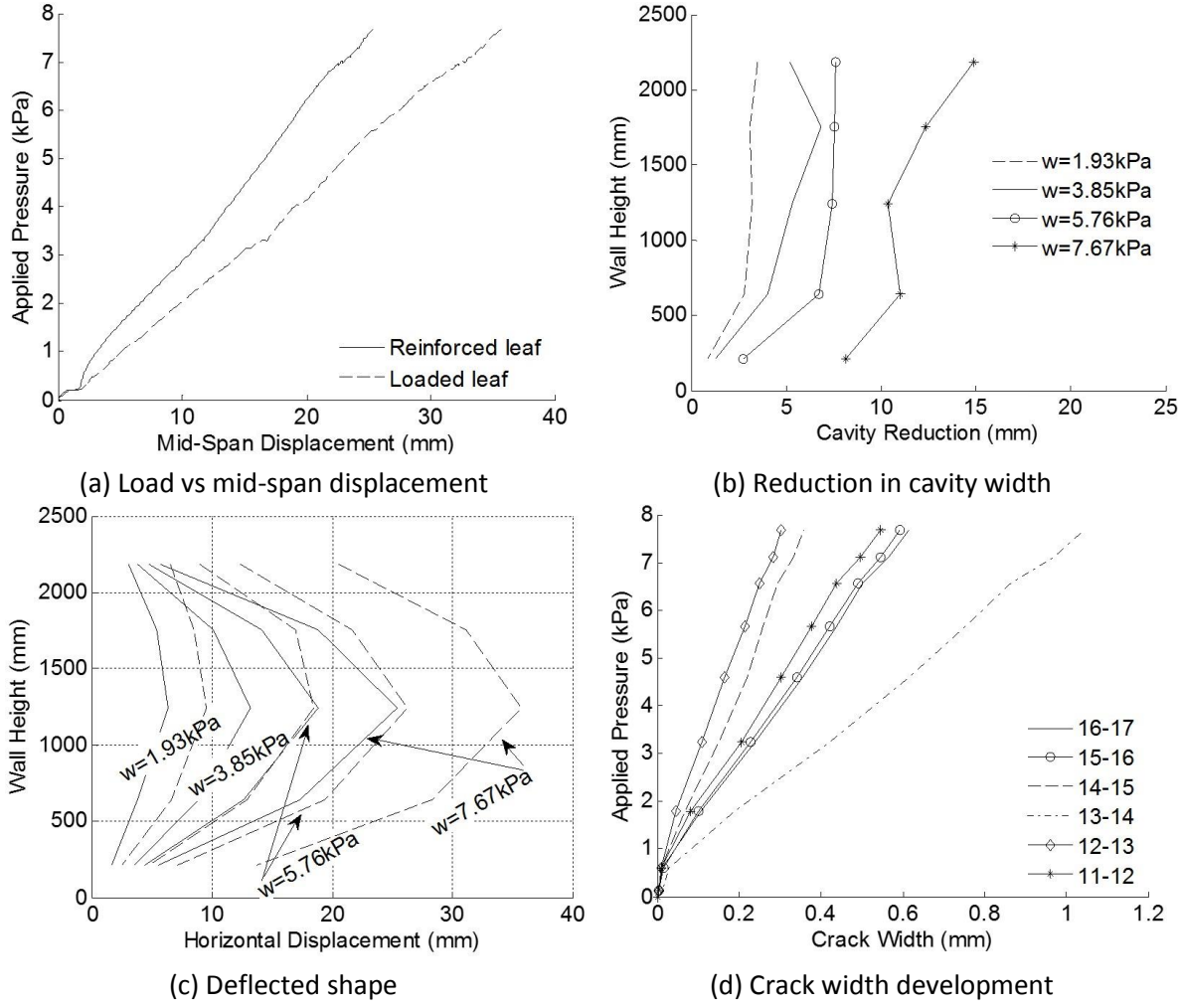

(a) Load vs mid-span displacement

(b) Reduction in cavity width

(c) Deflected shape

(d) Crack width development

Figure 17: Wall 5 test results

5.6. W6 - Cavity Wall, Mechanical Anchorage 2

The 6th wall test reused the pre-cracked wall from wall tests 3 and 5 and was designed to investigate the mechanical wall anchors while improving on the problems identified during the 5th wall test. In an effort to maintain the cavity dimension and minimize the likelihood of lateral buckling, the number of anchors was doubled with 2 anchors installed at each level near the edges of the masonry wall (Figure 4(a)). Testing of the 6th wall was undertaken on the 23th of February 2016 in the Chapman Laboratory at The University of Adelaide (Figure 18).

Figure 20(a) shows the load vs mid-height displacement response of wall test where the 'blue' line shows the mid-height deflection of the R reinforced leaf and the 'green' line shows the mid-height deflection of the airbag loaded leaf. Again the pre-loading of the test wall results in immediate

reopening of the cracks in the mortar joints (Figure 20(d)) and the linear load-deflection behavior throughout the entire test range.

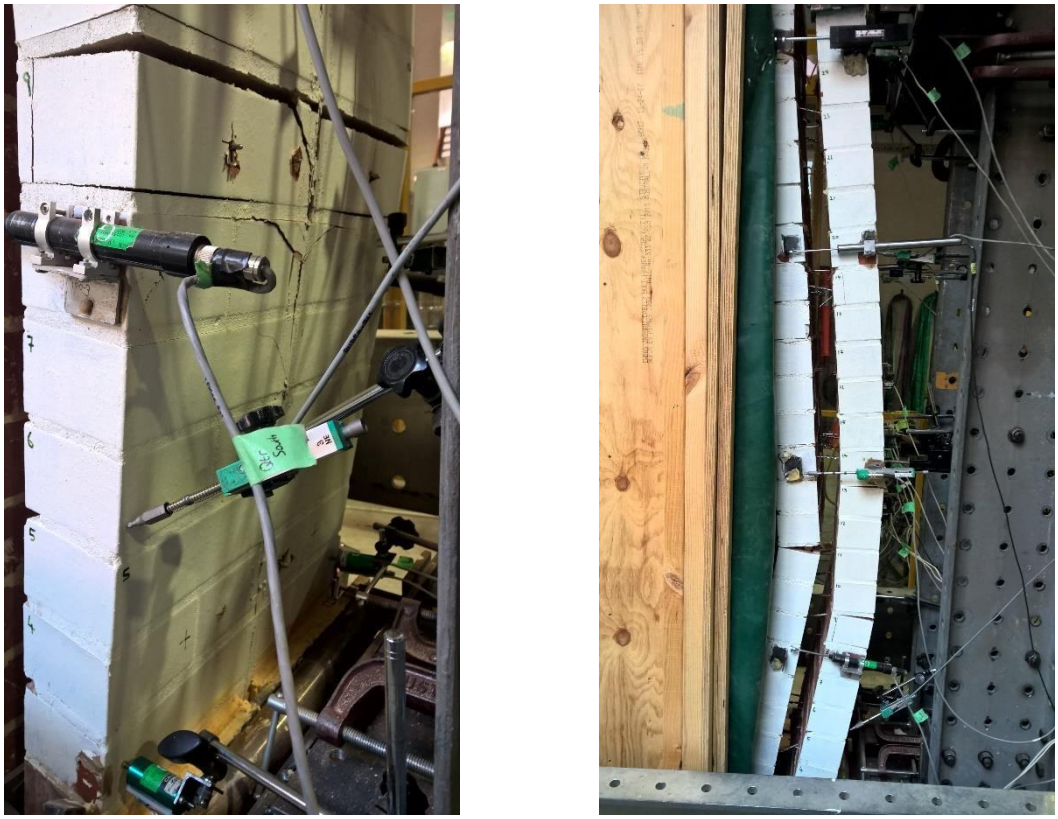

(a) IC debonding of FRP strip (b) Collapse of cavity width

Figure 18: Wall 6 final cracking pattern

Wall test 6 achieved global IC debonding at a pressure of 14.4 kPa corresponding to a failure of the tensile retrofitting of the masonry wall. Global debonding of the FRP strip occurred from the flexural crack located between the 9th and 10th courses and progressed to the base of the masonry wall (Figure 18(a)). As observed in the single leaf wall test, inspection of the FRP strip indicated that failure occurred in the surface layer of the FRP strip rather than the typically observed failure of the masonry substrate. However the presence of the herringbone crack formations indicated that the failure loads for the FRP strip and masonry substrate are reasonably close.

5.1. W7 - Cavity Wall, Foam Infill

Testing of the 7th wall was undertaken on the 17th of September 2015 in the Chapman Laboratory at The University of Adelaide. The 7th wall test reused the pre-cracked wall from wall test 4 and was designed to investigate the use of self-expanding foam as a method of transferring compression loads between the masonry leaves. In the case of wall test 7 the cavity was completely filled with foam (Erathane TX56) to create a sandwich panel consisting of FRP reinforced masonry skins and a foam core (Figure 19(a)).

Interestingly while the mechanical anchors didn't buckle there was a still a significant reduction in the cavity width as evident in Figure 20(b) and Figure 18(b). This reduction was again accommodated by the mechanical anchors being pushed out of the reinforced leaf.

(a) Foam cored cavity wall

(b) Foam induced crack expansion

Figure 19: Wall 7 damage prior to testing

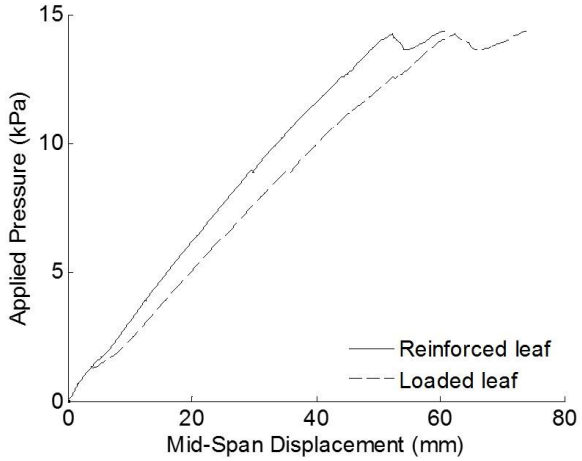

(a) Load vs mid-span displacement

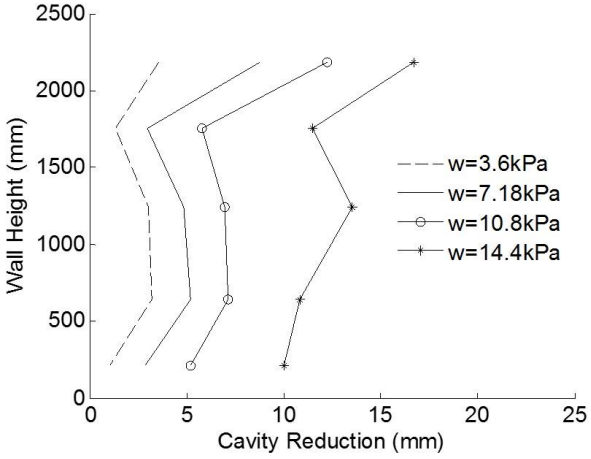

(b) Reduction in cavity width

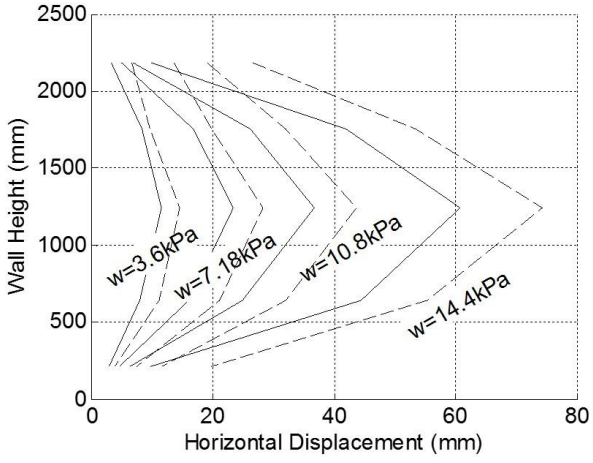

(c) Deflected shape profile

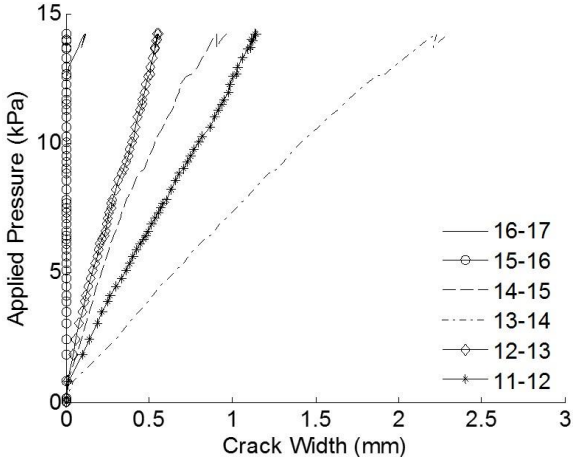

(d) Crack width development

Figure 20: Wall 6 test results

During installation of the foam several potential complications were identified for use in a real world environment. Firstly the foam selected was found to be quite viscous for several minutes after initial mixing after which there was a period of rapid foam expansion. Using the foam during the viscous period meant that the wall had to be sealed to prevent the liquid draining from the base of the wall. Waiting for the foam to start its expansion introduced a major time constraint on the installation process and the rapid expansion significantly increased the difficulty of the installation.

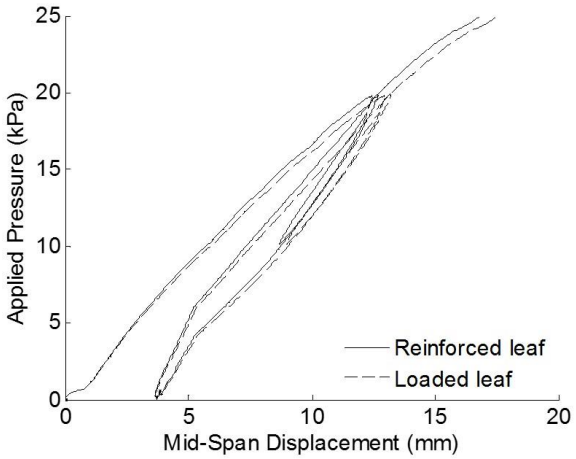

(a) load vs mid-span displacement

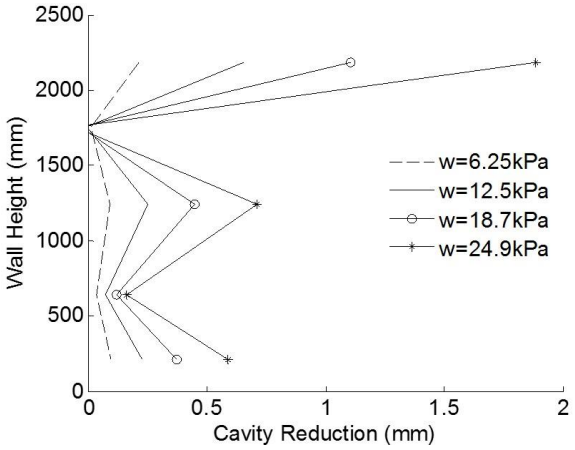

(b) reduction in cavity width

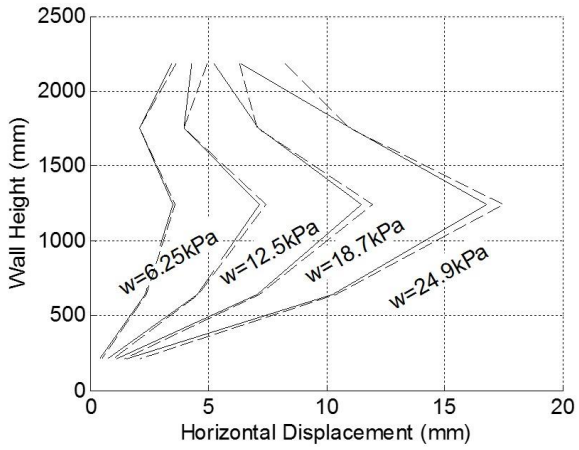

(c) wall deflected shape

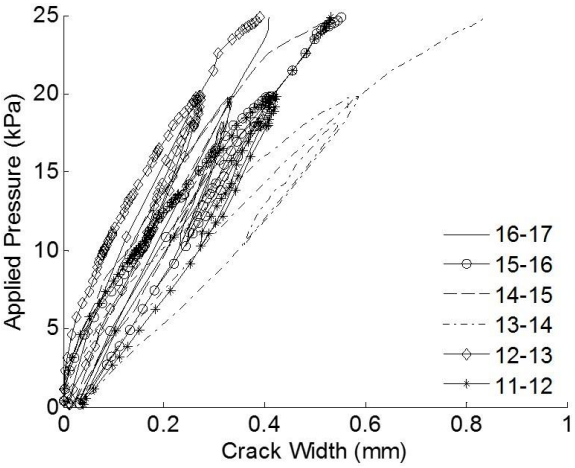

(d) crack width development

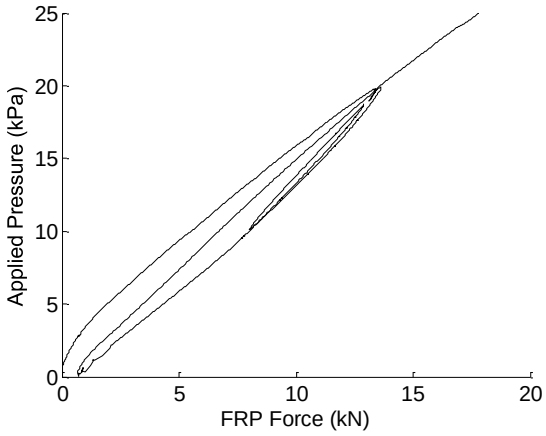

(e) measured FRP force

Figure 21: Wall 7 test results

Secondly as the wall was pre-cracked from previous testing, the pressure induced by the expanding foam resulted in bowing of the masonry leaves apart and increasing the cavity width. Additionally the foam in its viscous state was able to flow into the preexisting cracks and the subsequent expansion resulted in further opening of the cracks and the corresponding wall deflections (Figure 19(b)). Both of these problems could be addressed by the selection of a more suitable foam with reduced viscosity and through propping of the walls to prevent any unintended expansion damage.

Figure 21(a) shows the load to mid-height deflection profile for wall test where the 'blue' line shows the mid-height deflection of the R reinforced leaf and the 'green' line shows the mid-height deflection of the airbag loaded leaf. Again the pre-loading of the test wall resulted in immediate reopening of the cracks in the mortar joints (Figure 21(d)) and a linear load-deflection behavior throughout the entire test range.

Wall test 7 demonstrated the significant increase in strength achievable using the expanding foam as a connection method within the cavity. Wall 7 was subjected to an applied pressure of 24.9 kPa which was the upper limit that could be applied using the designed test rig. At this load it was found that there was a negligible reduction in the cavity width (Figure 21(b)).

The creation of a solid sandwich panel resulted in a significant increase in both strength and stiffness of the test wall over the other test walls such that at the maximum applied pressure of 24.9 kPa (a 180% increase over Wall 3) the mid-span deflection was only 16.8 mm (a 40% reduction compared with Wall 3). This increase in stiffness resulted in decreased crack widths (Figure 21(d)) and subsequently a reduction of the load in the FRP strip (Figure 21(e)). If the wall had been pushed further it is likely that the crack widths would have opened sufficiently for IC debonding to have been the ultimate failure mechanism however the displayed increase in strength could potentially indicate that a foam core could provide a significant increase in wall strength without the need for additional tensile strengthening.

5.1. W8 - Cavity Wall, Foam Channel

The 8th wall test consisted of an FRP reinforced cavity wall where the existing wall tie connection between the masonry leaves was cut and replaced with a nominally 50mm deep channel of foam on each side of the strip wall. Testing was undertaken on the 14th of April 2016 in the Chapman Laboratory at The University of Adelaide. The general test setup for the test wall is shown in Figure 22(a) and a close-up of the foam channel is shown in Figure 22(b).

Installation of the foam channels involved placing a sacrificial 3 mm thick section of cardboard across the full width of the cavity at a distance of 50mm from the edge of the wall (Figure 22(b). An off the shelf variety of non-structural foam-in-a-can (Sika® Boom-AP) was then applied in a 10 mm bead on each side of the channel. This was left to set for 2 hours before additional foam was added to fill the cavity. Once the foam had set a hand saw was used to cut the excess foam from the wall.

The testing of the NSM FRP reinforced foam channel followed a similar behavior to that observed with the closely spaced wall ties of the 4th test wall. That is, by the later stages of loading the NSM reinforced leaf displayed horizontal hairline cracks at every mortar joint while the loaded leaf was dominated by the formation of cracks between the 9th-10th and 12th-13th courses. At an applied pressure of 18.9 kPa the foam around the top support reached its compressive capacity and gradually crushed resulting in

a significant reduction in the cavity width (Figure 22(c)). Further loading resulted in IC debonding of the NSM reinforcement at a mid-height displacement of 58 mm and reduced loading of 14.8 kPa. Debonding of the NSM reinforcement induced a sudden increase in the crack width between the 18th19th courses in the reinforced leaf and the 17th-18th courses in the loaded leaf.

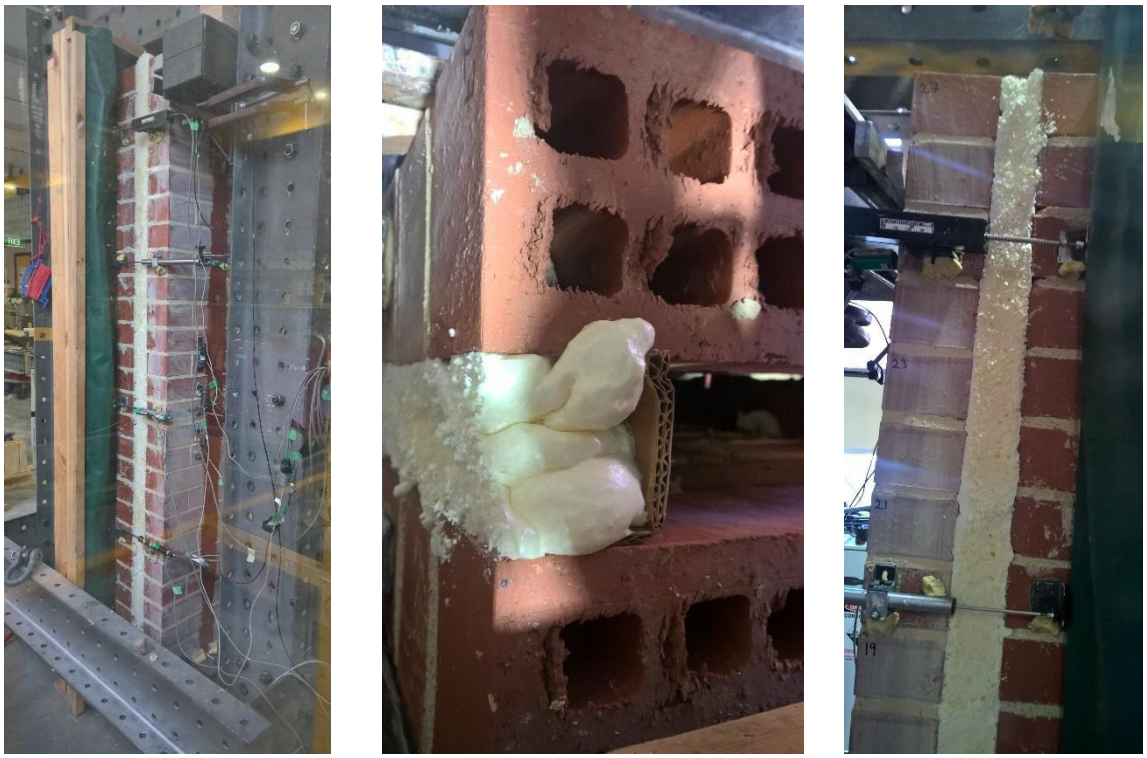

(a) Overall test configuration (b) foam channel (top view) (c) Foam compression at top support during testing Figure 22: Wall 8 foam details and cavity gap reduction during testing

Figure 23 shows the load vs mid-height deflection profile where the 'blue' line shows the mid-height deflection of the front, unreinforced leaf and the 'green' line shows the mid-height deflection of the airbag loaded leaf. Figure 23(a) shows that the loaded leaf follows closely the path of the front, unloaded leaf and shows that the foam was capable of maintaining the cavity width at mid-height. Near the supports, however, the foam was gradually compacted such that, on achieving the maximum resisted 18.9 kPa, the cavity width had reduced by 10 mm (Figure 23(b)). Figure 23(c) shows the horizontal deflection profile of the wall at various applied loads. In Figure 23(c) the solid line corresponds to the deflection of the reinforced leaf and the dashed line shows the deflection of the loaded leaf. From this figure it can be seen that both leaves rotated, such that just below the support a displacement of 5 mm was achieved, before the wall engaged the top support.

Figure 23(d) shows the crack width development near mid height of the front leaf. For this test it appears that significant crack growth did not begin until an applied pressure of 3.0 kPa was achieved. It is also interesting to note that unlike the wall tie connections or mechanical anchorage connections of test walls 3 through 6, the initiation of crack growth did not result in a sudden change in behavior but rather a gradual reduction in stiffness as evident in Figure 23(a).As demonstrated by the recorded

crack widths in Figure 23(d) horizontal cracks had formed at each of the 6 central mortar joints prior to a pressure of 7.0 kPa being applied to the wall.

The development of force in the NSM FRP strip is shown in Figure 23(e). Once again it can be seen that it is not until after the formation of flexural cracks at an applied pressure of 3.0 kPa that the FRP strip is utilized. It is also interesting to note that the force in the FRP strip continues to increase following compressive failure of the foam at an applied pressure of 18.9 kPa. This shows how the force in the FRP strip is tied to the growth of the crack widths and not the applied pressure. In the case of this test wall, the force in the FRP continued to increase to a load of 40 kN at which point IC debonding occurred. This debonding load is consistent with the 44 kN achieved in the FRP strip from the first wall test (Figure 8(d)). It is worth noting that in both cases the horizontal crack associated with debonding was located 3-4 courses away from the strain gauges attached to the FRP strip and may not be an accurate reflection of the max force in the FRP strip which would be expected to occur at the location of the dominant horizontal crack.

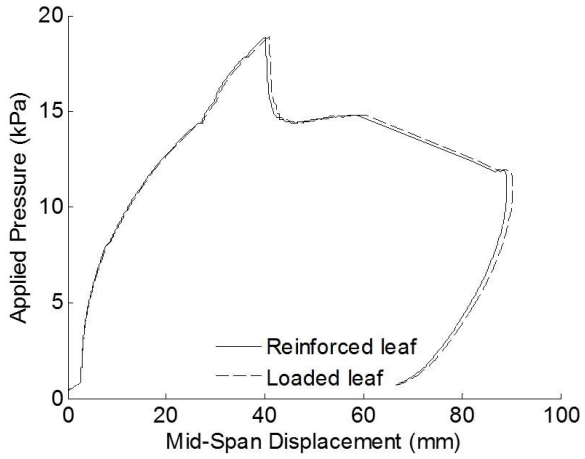

(a) Load vs mid-span displacement

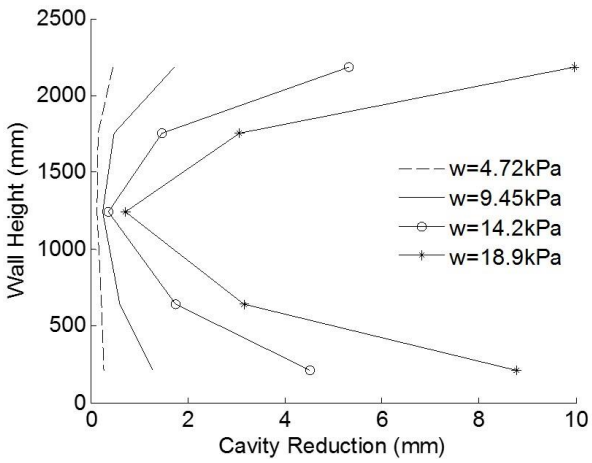

(b) Reduction in cavity width

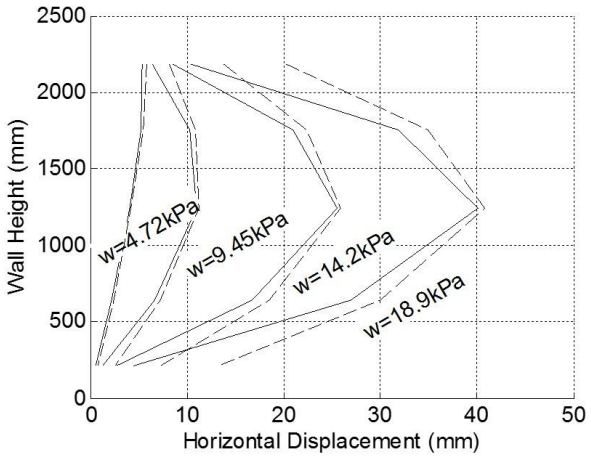

(c) Deflected shape profile

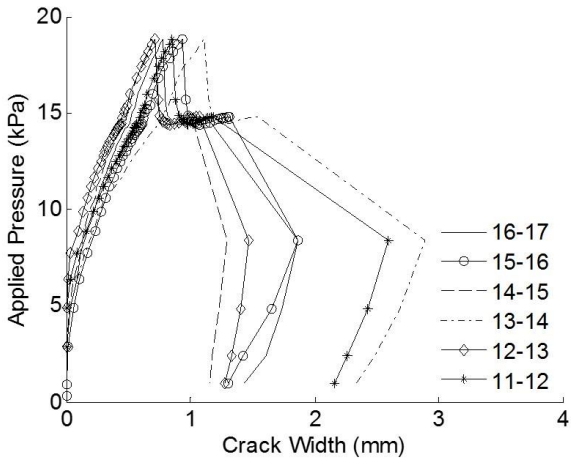

(d) Crack width development

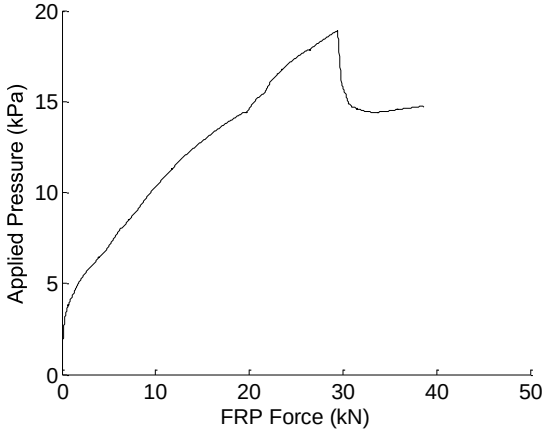

(e) FRP force development

Figure 23: Wall 8 test results

5.2. W9 - Cavity Wall, Foam Channel, No FRP

The 9th wall test consisted of an unreinforced cavity wall, i.e. no FRP, where the existing wall tie connection between the masonry leaves was cut and replaced with a nominally 50mm deep channel of foam on either side of the strip wall. Testing was undertaken on the 28th of April 2016 in the Chapman Laboratory at The University of Adelaide. The general test setup for the test wall is shown in Figure 24(a) and a close-up of the foam channel is shown in Figure 24(b).

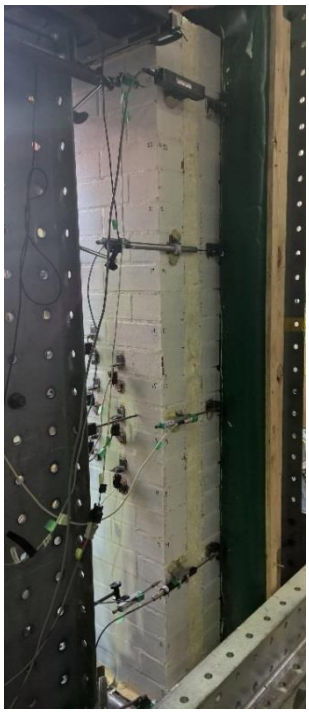

(a) Overall test configuration

(b) Foam cavity

(c) Flexural failure

Figure 24: Wall 9 cracking pattern

The purpose of this test configuration was to determine the strength improvement that could be achieved using foam alone and hence determine the contribution provided via the FRP reinforcement. Installation of the foam channels was identical to that for the 8th wall test and involved placing a sacrificial 3 mm thick section of cardboard across the full width of the cavity at a depth of 50mm (Figure

24(b)) which was then filled with an off the shelf variety of non-structural foam-in-a-can (Sika® Boom-AP). Once the foam had set a hand saw was used to cut the excess foam from the wall.

The testing of the 9th wall followed a similar behavior to that observed with the 2nd wall test where no reinforcement was present. Specifically the testing of the unreinforced, foam channel cavity wall was dominated by the formation of 3 horizontal cracks. A single crack formed in the front, unloaded leaf between the 18th-19th courses and the remaining 2 cracks formed in the loaded leaf between the 17th18th and 19th-20th courses as shown in Figure 24(c). Subsequent loading resulted in increased deflections, accommodated by the growth of these 3 cracks, with minimal increase in the resisted pressure. From Figure 24(c) it can also be seen that the foam channel enabled the wall cavity wall to achieve composite action with the flexural crack progressing through the front, unloaded wall and into the foam channel.

Figure 25(a) shows the load to mid-height deflection profile for the 9th test wall where the 'blue' line shows the mid-height deflection of the front, unreinforced leaf and the 'green' line shows the midheight deflection of the airbag loaded leaf. It should be noted that the initial deflection prior to 2 mm was caused by a rotation of both wall leaves such that good contact was made with the top roller support at the 26th course. This initial rotation displacement is exaggerated with wall height as can be seen by the blue line in Figure 25(c).

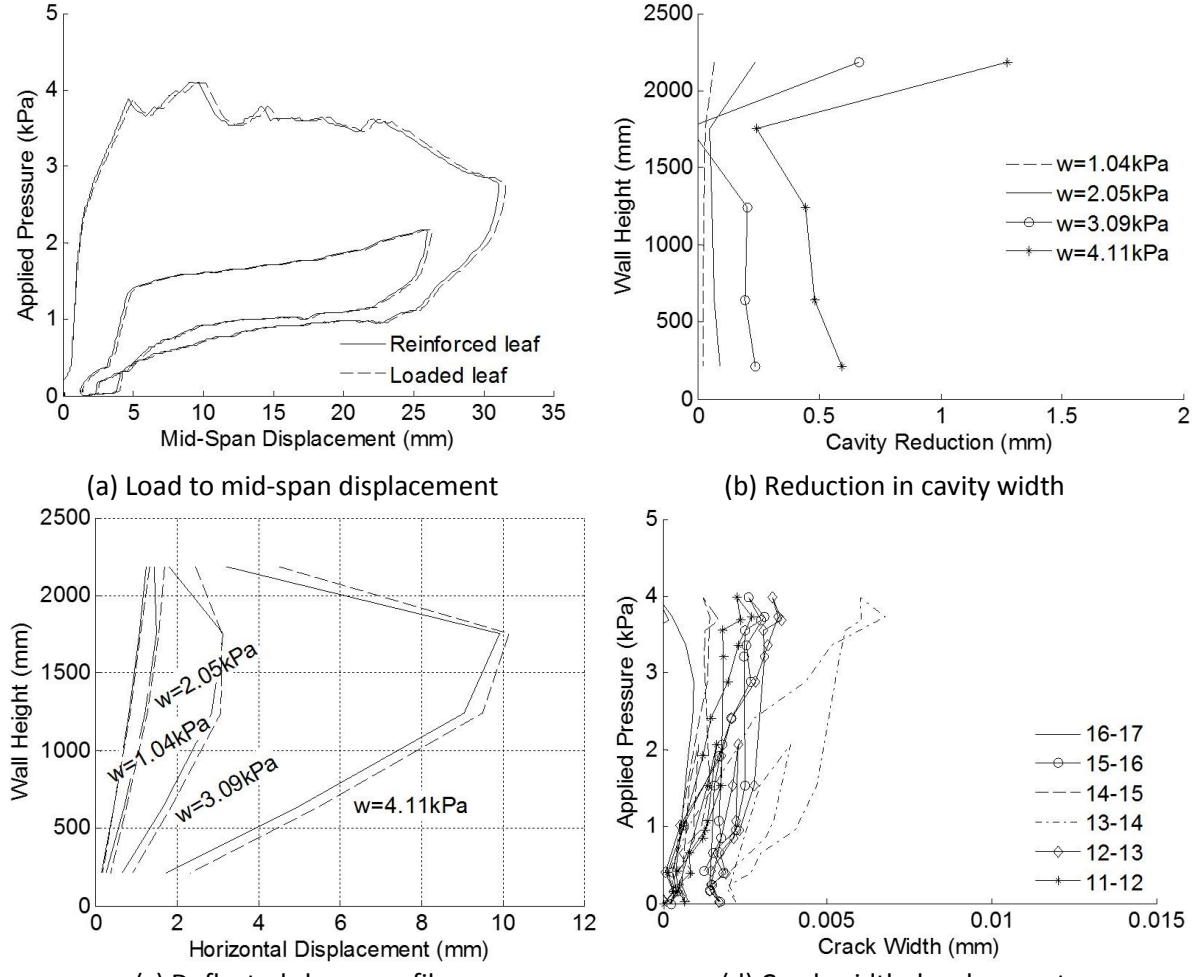

(a) Load to mid-span displacement

(b) Reduction in cavity width

(c) Deflected shape profile

(d) Crack width development

Figure 25: Wall 9 test results

Figure 25(a) shows that the loaded leaf follows closely the path of the front, unloaded leaf and demonstrates that the foam channels were capable of maintaining the cavity width at mid-height. This observation is further highlighted in Figure 25(b) which shows that the maximum reduction in the cavity width prior to achieving the maximum applied load was 1.5 mm at the top of the wall. Figure 25(c) shows the horizontal deflection profile of the wall at various applied loads. In Figure 25(c) the solid line corresponds to the deflection of the reinforced leaf and the dashed line shows the deflection of the loaded leaf. Once again this clearly shows that the foam channels were able to maintain the cavity dimensions up to the maximum applied load. Finally, Figure 11(d) shows the crack width development near mid height of the front loaded leaf. From Figure 25(d) is can be seen that none of the instrumented mortar joints near wall mid-height developed any flexural cracking.

4. Discussion of results

The backbone curve for the recorded force-displacement data of the unretrofitted wall W2 is separately shown in Figure 26, with Figure 27 showing the backbone curve for the walls retrofitted using different techniques. The plotted data represent the part of the tests during which the cavity gap was maintained by the ties, and the ties/anchors failed under forces beyond that shown in these plots.

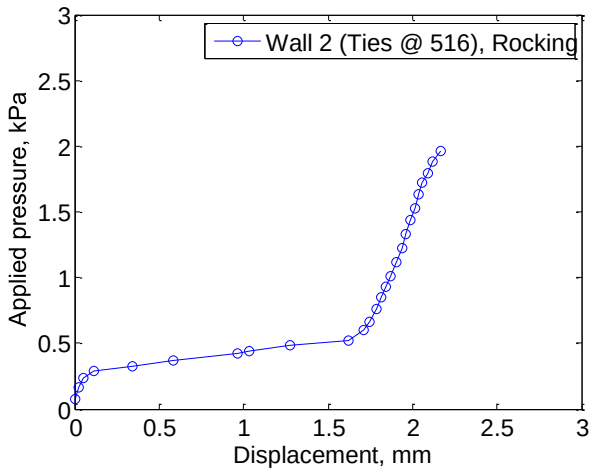

Figure 26: Applied pressure vs max displacement response of the unretrofitted cavity wall 2

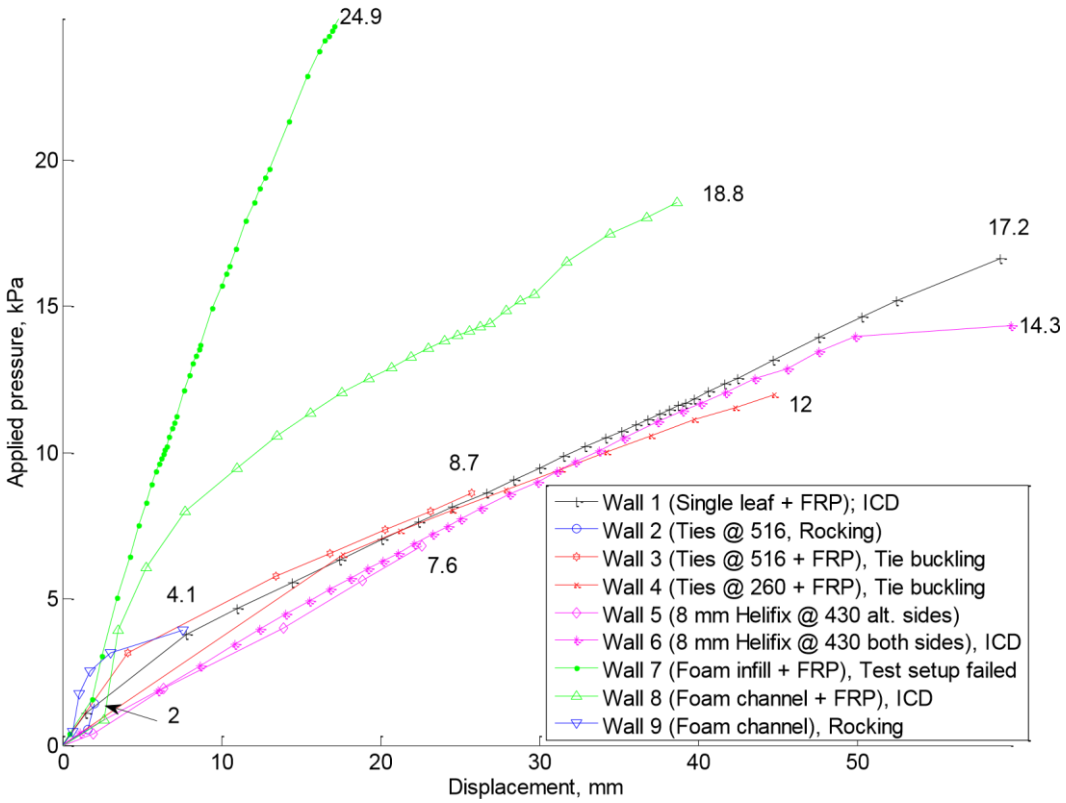

Figure 27: Applied pressure vs max displacement response of the tested walls

From Figure 26, it can be seen that the as-built anchors cannot maintain the cavity gap for applied pressures up to approximately 2 kPa, which corresponds to a lateral acceleration of 0.5g applied on a

top-storey cavity wall. The AS1170.4 (2007) stipulates that out-of-plane loaded walls need not be designed for 0.5g applied acceleration. This acceleration corresponds to a seismic Hazard factor of Z=0.14 (AS1170.4) and shallow soil. Although this hazard factor is greater than the hazard factor in most regions in Australia, the results from this single test is insufficient to conclude that no retrofit is required for existing walls. Experiences have shown that variability in construction practice is an important factor when dealing with URM walls. In addition, this strength corresponds to a factor of safety of 0.14/0.10=1.4 for Adelaide (Z=0.10). This factor of safety is less than that implied by capacity reduction factor for flexure in AS 3700 (1/0.6=1.67).

From Figure 27, it can be seen that all of the retrofitted walls, except for Wall 9 (foam strips but no FRP), significantly increased the wall strength, and the increase was at least 280% (i.e. 7.6 kPa for Wall 5 vs. 2 kPa for Wall 2). With this increased strength the walls will satisfy seismic requirements in Australia with acceptable safety factor.

It can be seen from the plots in Figure 27 that the two walls that were retrofitted using foam + FRP had the greatest initial stiffness, but the initial stiffness of other retrofitted walls were almost the same. From the two walls with foam contribution, the one that had foam strips had its stiffness reduced with the increase in the applied load, with the residual stiffness appearing to be of the same magnitude as that of the walls with anchor/tie + FRP.

Concluding solely based on the F-□ curves, the wall fully infilled with foam + FRP (Wall 7) had the best performance, but that wall also underwent some damage due to expanding foam penetrating through the mortar joints because of the confinement. Foam strips appear to be a more suitable option although its application to real walls may be impractical. Its application may need the removal of roof linings and access to the cavity gap from above, which increases retrofit costs. Tests should be done that investigate the properties of the foam that can be employed to successfully inject from outside the wall through holes that are created in one wall skin. There is a possibility that a specific density and viscosity of foam can be established for this purpose.

In lieu of more information about the practicality of the use of foam for retrofit, it is recommended to use anchors + FRP option as this retrofit method (Wall 6) also was successful. It should be noted that if limited anchors are used, e.g. Wall 5, the wall may prematurely fail due to anchor buckling.

5. Summary and conclusions

A total of 9 out-of-plane URM wall tests were completed at the University of Adelaide to investigate the effectiveness of different seismic retrofit options for URM cavity walls. The retrofit methods included NSM FRP installed on one wall skin and an improvement of the cavity ties by means of increased tie density, mechanical anchorage with different density, or foam infill with two different configurations.

The results showed that ties or foam alone cannot satisfactorily increase the wall out-of-plane strength, but that if these configurations are accompanied by NSM FRP on external wall surfaces, then the wall will satisfy the expected seismic demands for regions in Australia.

In summary from different tests, it was concluded that:

- Standard ties or foam strips alone (no NSM retrofit) are not suitable options.

- Walls with standard ties or mechanically installed helical ties will develop gains in strength sufficient to satisfy the expected seismicity (AS1170.4:2007) in Australian capital cities if NSM FRP retrofit is applied to the external wall faces. The wall strength will be governed by either ties buckling (larger spacing) or FRP IC debonding (smaller spacing).

- Fully foam-infilled walls may be prone to damage during the retrofit and before earthquake loading so that this seismic intervention may be unsuitable.

- Expanding foam strips provided satisfactory results, i.e. maintaining the gap for load increases that allowed the wall to develop full debonding strength. The only concern about this method at this time is developing an economical way of the application. This aspect needs to be studied by varying the chemical and physical properties, e.g. density and viscosity, of the foam liquid and injecting the foam from the outside the wall without the need to access to the cavity from the above. The latter requires removal of roof in real building, and the practice may be expensive.

6. References

De Lorenzis, L. & Teng, J. G. (2006 . “Near-surface mounted FRP reinforcement: An emerging technique for strengthening structures.” *Composites Part B: Engineering*, doi:10.1016/j.compositesb.2006.08.003

Ingham, J., & Griffith, M. C. (2010). “Performance of unreinforced masonry buildings during the 2010 Darfield (Christchurch, NZ) earthquake.” *Australian Journal of Structural Engineering*, 11(3), 207-224.

Griffith, M. C. . “Performance of unreinforced masonry buildings during the Newcastle Earthquake, Australia.” Research Report No. R86, Department of Civil Engineering, University of Adelaide, Australia.

Hamed, E., & Rabinovitch, O. (2010). “Failure characteristics of FRP-strengthened masonry walls under out-of-plane loads.” *Engineering Structures*, *32*(8), 2134-2145.

Ghobarah, A., & El Mandooh Galal, K. (2004). “Out-of-plane strengthening of unreinforced masonry walls with openings.” *Journal of Composites for Construction*, *8*(4), 298-305.

Griffith, M. C., Kashyap, J., & Mohamed Ali, M. S. (2013). “Flexural displacement response of NSM FRP retrofitted masonry walls.” *Construction and Building Materials*, *49*, 1032-1040.

Kashyap, J., Griffith, M. C., Mohamed Ali, M. S., & Oehlers, D. J. (2011). “Prediction of load-slip behavior of FRP retrofitted masonry.” *Journal of Composites for Construction*, *15*(6), 943-951.

Kashyap, J., Willis, C. R., Griffith, M. C., Ingham, J. M., & Masia, M. J. (2012). “Debonding resistance of FRP-to-clay brick masonry joints.” *Engineering structures*, *41*, 186-198.

Khalifa, A. M. (2016). “Flexural performance of RC beams strengthened with near surface mounted CFRP strips.” *Alexandria Engineering Journal*.

Korany, Y. and Drysdale, R. . “Rehabilitation of Masonry Walls Using Unobtrusive FRP Techniques for Enhanced Out-of- lane Seismic Resistance.” *J. Compos. Constr.*, 10.1061/(ASCE)10900268(2006)10:3(213), 213-222.

Oehlers, D., Visintin, P., and Lucas, W. (2015). "Flexural Strength and Ductility of FRP-Plated RC Beams: Fundamental Mechanics Incorporating Local and Global IC Debonding." *J. Compos. Constr.*, 10.1061/(ASCE)CC.1943-5614.0000610, 04015046.

Visintin, P., Oehlers, D. J., Muhamad, R., & Wu, C. (2013). “Partial-interaction short term serviceability deflection of RC beams.” *Engineering Structures*, 56, 993-1006.

Walsh, K. Q., Dizhur, D. Y., Shafaei, J., Derakhshan, H., & Ingham, J. M. (2015, August). “In Situ Outof-Plane Testing of Unreinforced Masonry Cavity Walls in as-Built and Improved Conditions.” In *Structures* (Vol. 3, pp. 187-199). Elsevier.

Willis, C. R., Yang, Q., Seracino, R., & Griffith, M. C. (2009). “Bond behaviour of FRP-to-clay brick masonry joints.” *Engineering Structures*, *31*(11), 2580-2587.

AS 3700 (2011). Australian Standards for Masonry Structures. Standards Australia International, Sydney, NSW 2001, Australia.

AS 4456 (2003). Masonry units, segmental pavers and flags—Methods of test. Standards Australia International, Sydney, NSW 2001, Australia

AS 1170.4 (2007). Structural design actions. Part 4: Earthquake actions in Australia. Standards Australia International, Sydney, NSW 2001, Australia